AFOSR-TR- 80-0627

LEVEL II

(5)

ANNUAL TECHNICAL REPORT

1 October 1978 - 30 September 1979

ARPA Order: 3291-21

Program Code: 9D60

Contractor: The Regents of the University of California
University of California, San Diego
La Jolla, California 92093

Effective Date: 1 October 1978

Expiration Date: 30 September 1979

Amount of Contract: $91,397

Contract Number: F49620-79-C-0019

Principal Investigators: L. M. Dorman (714) 452-2406
J. A. Orcutt (714) 452-2887
T. H. Jordan (714) 452-2809

Program Manager: Mr. William J. Best

Title: Seismic Detection and Discrimination Using Ocean-Bottom Seismographs

Sponsored by: Advanced Research Projects Agency (DOD)
ARPA Order No. 3291-21

Monitored by: AFOSR under contract #F49620-79-C-0019

The views and conclusions contained in this document are those of the authors and should not be interpreted as necessarily representing the official policies, either expressed or implied, of the Defense Advanced Research Projects Agency or the U.S. Government.

Unclassified

SECURITY CLASSIFICATION OF THIS PAGE (When Data Entered)

REPORT DOCUMENTATION PAGE

READ INSTRUCTIONS BEFORE COMPLETING FORM

1. REPORT NUMBER: AFOSR-TR-80-0627	2. GOVT ACCESSION NO.: AD-A088 513
3. RECIPIENT'S CATALOG NUMBER:	
4. TITLE (and Subtitle): SEISMIC DETECTION AND DISCRIMINATION USING OCEAN-BOTTOM SEISMOGRAPHS	5. TYPE OF REPORT & PERIOD COVERED: Annual Technical Report, 10/1/78 - 9/30/79
	6. PERFORMING ORG. REPORT NUMBER: 1 Oct 78-30 Sep 79
7. AUTHOR(s): L. M. Dorman, J. A. Orcutt, T. H. Jordan	8. CONTRACT OR GRANT NUMBER(s): F49620-79-C-0019, ARPA Order-3291
9. PERFORMING ORGANIZATION NAME AND ADDRESS: Scripps Institution of Oceanography, University of California, San Diego, La Jolla, California 92093	10. PROGRAM ELEMENT, PROJECT, TASK AREA & WORK UNIT NUMBERS: AO 3291-21, 9D60
11. CONTROLLING OFFICE NAME AND ADDRESS: Defense Advanced Research Projects Agency, Nuclear Monitoring Research Office, 1400 Wilson Blvd., Arlington, VA 22209	12. REPORT DATE: Sep 79
	13. NUMBER OF PAGES: 41
14. MONITORING AGENCY NAME & ADDRESS (if different from Controlling Office): Air Force Office of Scientific Research/NP, Building 410, Bolling Air Force Base, Washington, D.C. 20332	15. SECURITY CLASS. (of this report): Unclassified
	15a. DECLASSIFICATION/DOWNGRADING SCHEDULE

16. DISTRIBUTION STATEMENT (of this Report)

Approved for public release; distribution unlimited.

17. DISTRIBUTION STATEMENT (of the abstract entered in Block 20, if different from Report)

18. SUPPLEMENTARY NOTES

19. KEY WORDS (Continue on reverse side if necessary and identify by block number)

Seismic noise
Ocean-bottom seismology
Discrimination
Instrumentation

20. ABSTRACT (Continue on reverse side if necessary and identify by block number)

Research progress on seismic detection and discrimination using ocean-bottom seismographs (OBS's) is outlined. During this first year of DARPA contract work, our investigations have been focused primarily on using existing OBS data to address the problem of sea-floor seismic noise and to constrain models of the near-bottom seismic environment. We have completed noise studies at six of our previously occupied OBS sites. The noise levels (cont.)

DD FORM 1 JAN 73 1473 EDITION OF 1 NOV 65 IS OBSOLETE
S/N 0102 LF 014 6601

Unclassified
SECURITY CLASSIFICATION OF THIS PAGE (When Data Entered)

Typical amplitude spectra roll off rapidly ~~(ω^{-4} ω^{-5})~~ out to 2-4 Hz and much less rapidly ~~(ω^{-2})~~ beyond 4 Hz. At frequencies above 4 Hz, the noise levels are low, typically a few nanometers/$Hz^{1/2}$ or less and comparable to good land-based stations. Several correlations between noise levels and other parameters, such as sediment thickness, distance from the continental margin and sea state, are discussed and used to constrain possible noise mechanisms. We hypothesize that the dominant mechanism of high-frequency (>2 Hz) noise generation at most of the sites examined thus far is of local oceanographic origin, exciting acoustic modes in the water column which couple to Stoneley modes at the sediment-water interface and waveguide modes within the sediment column. This hypothesis is supported by the analysis of noise data from two OBS arrays, which shows that the noise coherence is very low for pairs of sensors separated by as little as 200 m. We also outline some of the conclusions relevant to the seismic noise problem deduced by us from the data collected during the Lopez Island intercalibration experiment.

For the purpose of evaluating the detection and discrimination capabilities of OBS arrays, we have been analyzing the records obtained by a Scripps expedition to the Middle America Trench. Seismograms recorded off-shore from events in the Benioff zone show complexities not observed on land. Compressional phases multiply reflected within the water column form prominent later arrivals that can obscure body phases such as S, but the energy in these water multiples is concentrated at high frequencies and can be effectively removed by low-pass filtering. Substantial variations in low group-velocity modal amplitudes and frequencies are observed, and these correlate with sediment thickness.

Finally, we discuss our progress in investigations of triggering and recording strategies. The first step of our work has been to increase the sensitivity of the STA/LTA algorithm by tailoring the instrument response to the ambient noise spectrum prior to digitizing. We have also initiated an attack on the tape recording problem with the goal of increasing the total storage capacity significantly with no increase in error rate.

Table of Contents

List of Figures

List of Figures (continued)

Abstract

Research progress on seismic detection and discrimination using ocean-bottom seismographs (OBS's) is outlined. During this first year of DARPA contract work, our investigations have been focused primarily on using existing OBS data to address the problem of sea-floor seismic noise and to constrain models of the near-bottom seismic environment. We have completed noise studies at six of our previously occupied OBS sites. The noise levels of typical amplitude spectra roll off rapidly ($\sim\omega^{-4}$ - ω^{-5}) out to 2-4 Hz and much less rapidly ($\sim\omega^{-\frac{1}{2}}$) beyond 4 Hz. At frequencies above 4 Hz, the noise levels are low, typically a few nanometers/$Hz^{\frac{1}{2}}$ or less and comparable to good land-based stations. Several correlations between noise levels and other parameters, such as sediment thickness, distance from the continental margin and sea state, are discussed and used to constrain possible noise mechanisms. We hypothesize that the dominant mechanism of high-frequency (>2 Hz) noise generation at most of the sites examined thus far is of local oceanographic origin, exciting acoustic modes in the water column which couple to Stoneley modes at the sediment-water interface and waveguide modes within the sediment column. This hypothesis is supported by the analysis of noise data from two OBS arrays, which shows that the noise coherence is very low for pairs of sensors separated by as little as 200 m. We also outline some of the conclusions relevant to the seismic noise problem deduced by us from the data collected during the Lopez Island intercalibration experiment.

For the purpose of evaluating the detection and discrimination capabilities of OBS arrays, we have been analyzing the records obtained by a Scripps expedition to the Middle America Trench. Seismograms recorded off-shore from events in the Benioff zone show complexities not observed on land. Compressional phases multiply reflected within the water column form prominent later arrivals that can obscure body phases such as S; but the energy in these water multiples is concentrated at high frequencies and can be effectively removed by low-pass filtering. Substantial variations in low group-velocity modal amplitudes and frequencies are observed, and these correlate with sediment thickness.

Finally, we discuss our progress in investigations of triggering and recording strategies. The first step of our work has been to increase the sensitivity of the STA/LTA algorithm by tailoring the instrument response to the ambient noise spectrum prior to digitizing. We have also initiated an attack on the tape recording problem with the goal of increasing the total storage capacity significantly with no increase in error rate.

1. Introduction

The ocean-bottom seismometer (OBS) provides a sensitive, stable instrument platform for recording seismic waves on the two-thirds of the earth's surface covered by water. Modern OBS's, such as those operational or being constructed at Scripps, are capable of high-gain, broadband, multi-component, digital recording of regional events in deep water for extended periods of time. Because of these capabilities they should be useful for seismic detection and discrimination in regions inaccessible to conventional land-based instruments.

The purpose of the research outlined in this report is to provide data and analysis in support of DARPA's program for the deployment and operation of a Marine Seismic System (MSS) in the northwest Pacific Ocean.

At present many of the problems confronting ocean-bottom seismology are not well understood. Some of the important questions include: What are the spectral characteristics of seismic noise in the deep ocean basins? How is this noise generated and how does it vary in time and space? What is the response of a seismometer on the sediment-water interface to various incoming wave fields, and how does this response depend upon sub-bottom stratification and depth of sensor enplacement? Given the answers to these questions, then what is the optimal instrument design, and where should sensors be operated to yield seismographic data most useful for seismological studies of earthquakes and explosions? Finally, how should seismic data be collected on the sea floor and transmitted back to a land-based processing facility?

During this first contract period, our work has been focused primarily on using existing OBS data to address some of these questions and to constrain models of the near-bottom seismic environment.

2. Noise Studies

Records obtained by seismometers on the ocean floor show the presence of harmonic disturbances, ubiquitous in time and space, that are usually lumped under the rubric of seismic noise. The generation of ocean-bottom noise and its modes of propagation are not well understood, and most speculative discussions have lacked a foundation of quantitative data. We have begun a series of investigations into this problem and report here on our preliminary results.

Some typical examples of noise power spectra from a site at 15°N, 145°W (East Pacific Long Line Experiment) are shown in Figure 2.1. Acceleration spectra are given for three separate capsules deployed in an array with an aperture of about 2 km. The spectra for INEZ, GWEN and DOE, respectively, were obtained by stacking 52, 57 and 47 fast-Fourier transformed time series of 512 samples (4 sec) each. Each time series was tapered with a Hanning window and the mean was removed prior to transformation. The spectra have been corrected for instrumental response, so true ground acceleration is represented. The generally good consistency among the three estimates provides validation for the estimation procedure.

The strong roll-off of the seismic noise in the band 1-4 Hz is typical of deep ocean sites, as is the more gradual roll-off above 4 Hz. The data from other localities are discussed below.

For ocean-bottom sites near continent-ocean boundaries, surf beating may be an important mechanism, as documented on land (e.g., Phillips and McCowan, 1978). Surf beat and other distant sources of seismic noise (e.g., large storms) can be identified by frequency-wavenumber studies of noise coherence and propagation using arrays of seismometers (e.g., Haubrich and McCamy, 1969).

Other possible sources of noise include the local nonlinear interactions of ocean surface and internal waves propagated as acoustical disturbances in the water column (Hughes, 1976). Since these disturbances are primarily wind-driven, they can be identified by observing correlations between noise amplitude and surface-wind amplitude or sea

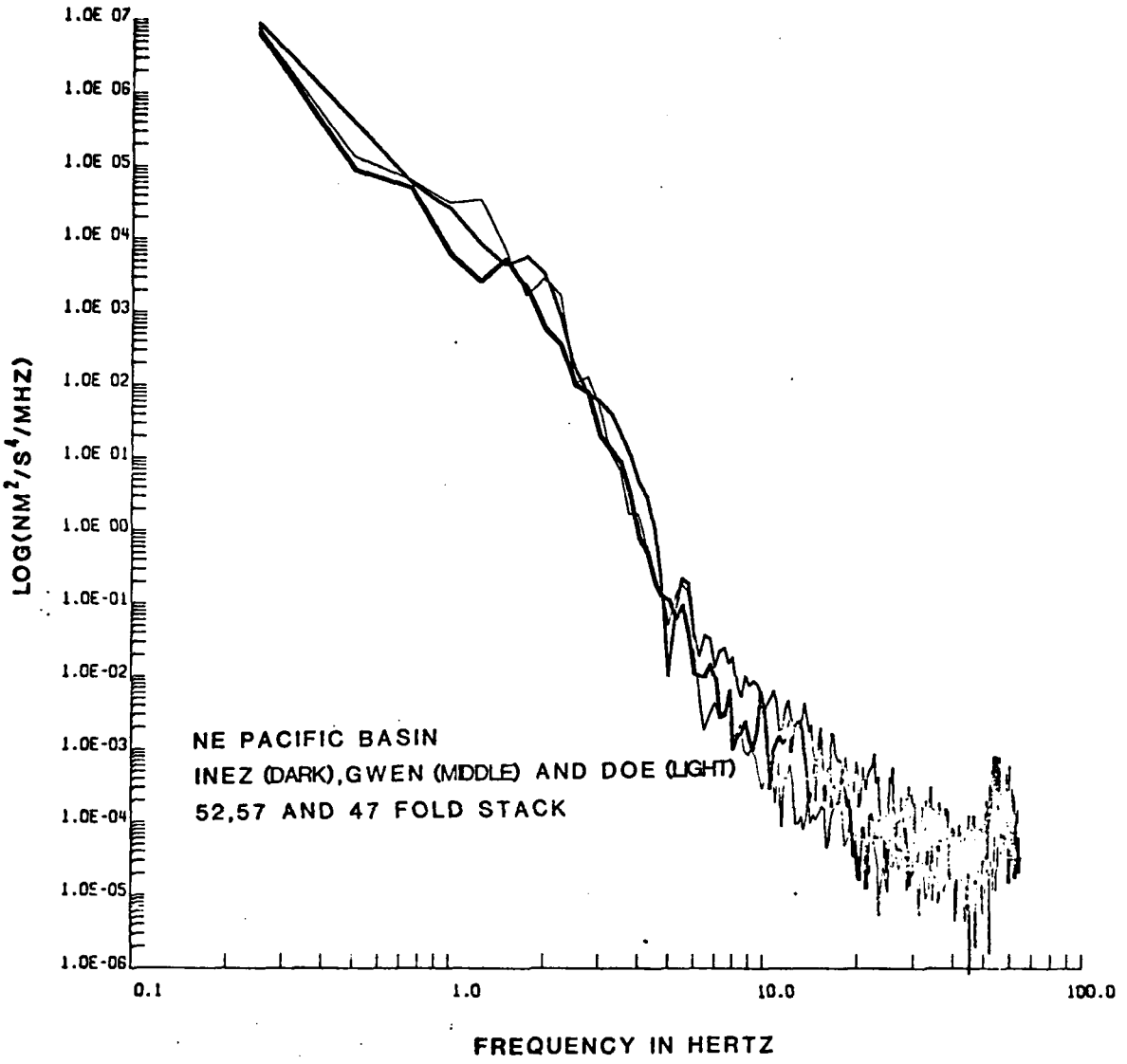

Figure 2.1. Acceleration power spectra from the East Pacific Long Line experiment for three OBS's. The spectra for INEZ, GWEN and DOE were obtained by stacking 52, 57 and 47 512-point (4-sec) transforms, respectively. The time series were tapered with a Hanning window and the mean was removed prior to transformation.

state. Because they are locally generated and vertically propagating, the coherence between neighboring seismometers should decrease rapidly with distance.

An even more localized source of noise involves the interactions of bottom currents with the OBS package itself. Currents of a few centimeters per second, which are not uncommon in the benthic boundary layer, can shed vorticies from the spherical pressure case of a Scripps-type OBS (Achenbach, 1974). Strong correlations between apparent seismic noise levels and local velocities measured on simultaneously deployed current meters should be diagnostic of this process. Because bottom currents are typically modulated by the tidal cycle, noise generated by this mechanism should also be tidally modulated.

2a. Geographic variations of sea-floor noise. We have completed noise studies at six of our previously occupied OBS sites; the locations are plotted in Figure 2.2. The abbreviations refer to the expeditions during which the original data were collected, and the numbers are the water depths in meters. The locality designations are:

1. Gorda Rise (GORDA)
2. East Pacific Long Line (EPLL)
3. Deepsonde II (DSII)
4. Middle America Trench (MAT)
5. Rivera Submersible Experiment (RISE)

The two depths at the MAT locality correspond to different seismometer sites in the trench axis (5500 m) and on the continental slope (3800 m).

The Scripps OBS is a digitally recording instrument with a variable memory buffer (4-12 sec) which captures a sample of bottom noise unsullied by the noise due to tape recorder operation. During an experiment the recorder is periodically turned on at pre-set intervals (with the option to trigger on large events), thus providing a number of samples of seismic noise.

Figure 2.3 illustrates a typical displacement amplitude spectrum from a moderately noisy site on the continental slope of the Middle American Trench. Amplitude spectra from other ocean-basin sites show similar characteristics. In most cases the noise level rolls off rapidly

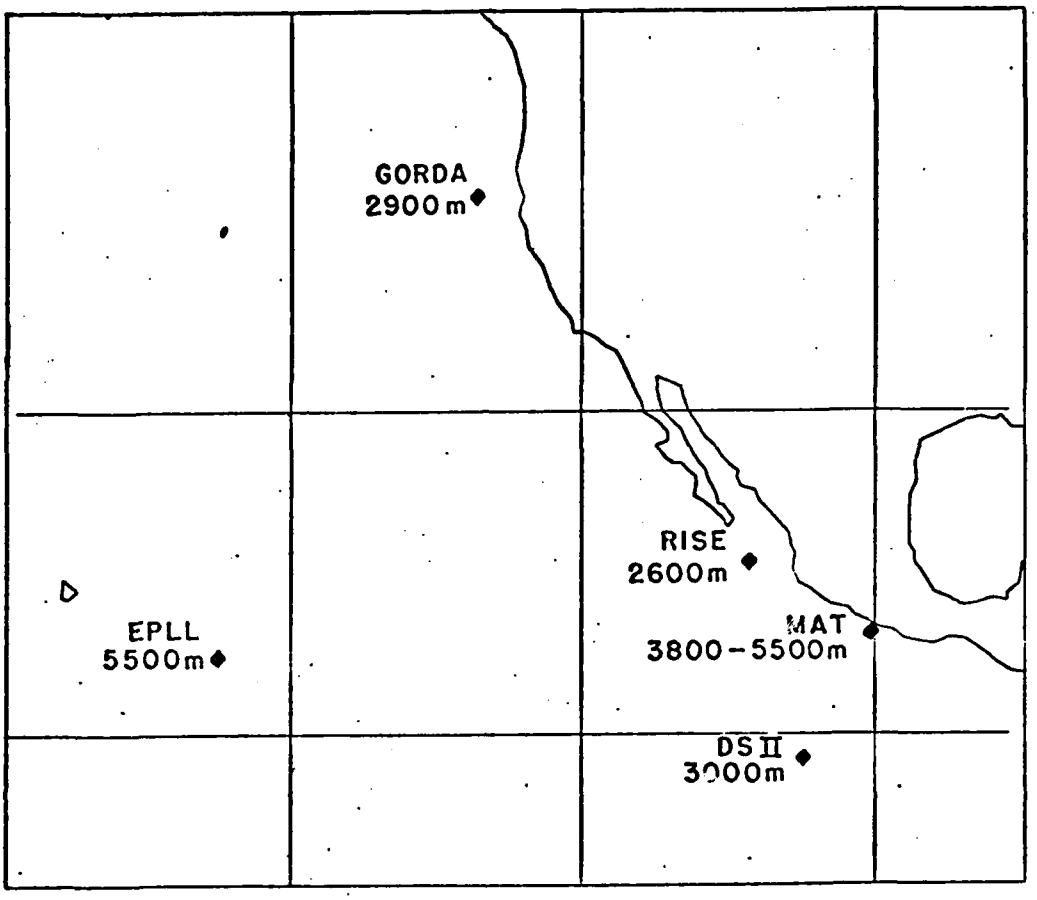

Figure 2.2. Scripps' Ocean Bottom Seismograph experiment sites included in this report. Water depths are shown in meters.

($\sim \omega^{-4} - \omega^{-5}$) out to 2-4 Hz and much less rapidly ($\sim \omega^{-1/2}$) beyond 4 Hz or so. At frequencies above 4 Hz, the noise levels are very low, typically a few units (nm/$Hz^{1/2}$) or less and comparable to good land-based stations.

Table 2.1 summarizes the noise spectra at all five sites. For each estimate several 10-s realizations were stacked to reduce the variance. The errors quoted are standard deviations of the spectra estimates. The sites are arranged in order of descending noise level.

Table 2.1. Summary of spectral amplitude measurements of seismic noise at several sites for 1, 4 and 10 Hz. (units are nanometers/$Hz^{1/2}$)

	1 Hz	4 Hz	10 Hz
GORDA RISE	767 ± 237	3.2 ± 1.5	1.17 ± 0.6
EAST PACIFIC LONG LINE	270 ± 92	1.6 ± 0.4	0.4 ± 0.1
DEEPSONDE II (9°N)	132 ± 34	1.4 ± 0.2	0.16 ± 0.02
MIDDLE AMERICA TRENCH: SEDIMENTARY WEDGE	110 ± 7	4.0 ± 0.1	1.1 ± 0.1
MIDDLE AMERICA TRENCH: TRENCH AXIS	60 ± 14	0.9 ± 0.5	0.4 ± 0.2
RISE (21°N)	56 ± 15	0.7 ± 0.1	0.2 ± 0.05

Several correlations (or lack thereof) relevant to the noise generation problem are suggested by the data in Table 2.1. It is interesting to note that both the noisiest site (GORDA) and the quietest site (RISE) were situated in nearly sediment-free environments on oceanic rise crests about equal distances from the continental margin. The differences in noise level are apparently due to differences in sea state: the GORDA experiment was conducted during rough weather conditions (sea state $\sim$ 5), whereas the RISE experiment occurred during very calm conditions (sea state $\sim$ 1)

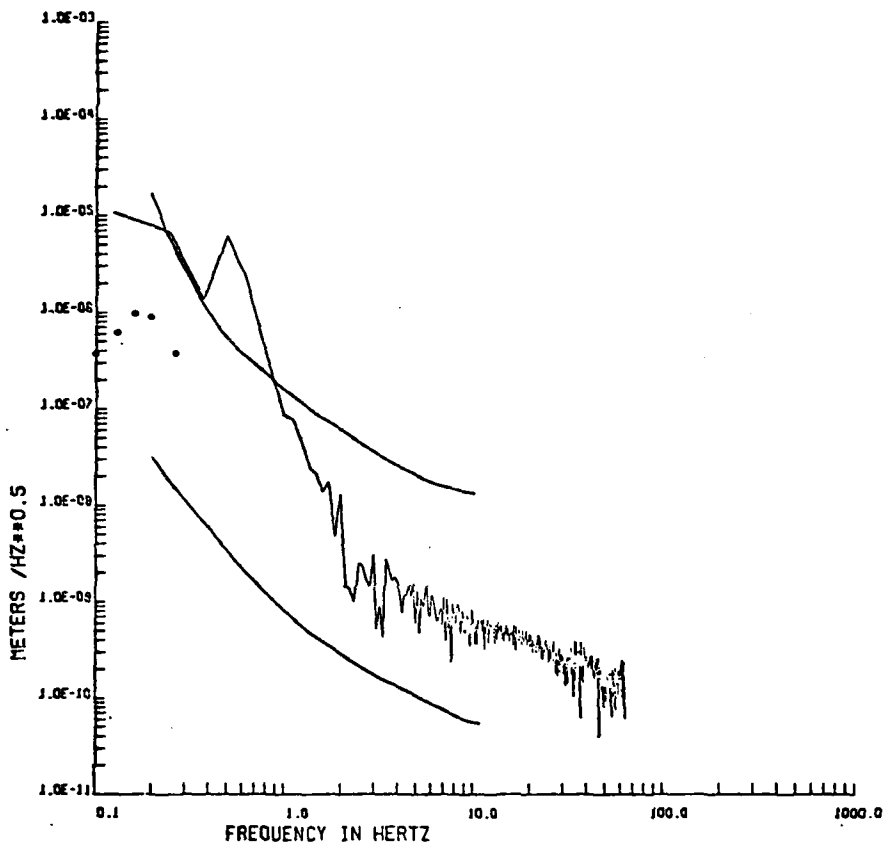

Figure 2.3. SIO noise spectrum from the Middle America Trench experiment compared to the high frequency Brune/Oliver limits on continental noise levels. The five dots at the low frequency end are measurements made nearly a decade ago in the Pacific basin by the SIO sea floor quartz fiber accelerometer.

There does appear to be a correlation between noise level and sediment thickness. For example, at the MAT sites, the noise levels were significantly higher on the sedimentary wedge than in the trench axis. With the notable exception of GORDA, the other sites obey this correlation. The analysis of earthquake records at these same sites clearly demonstrates that low-group-velocity Stoneley modes and organ-pipe modes are easily excited when the sediment thickness is large, suggesting that seismic noise may be concentrated in these modal components.

At the EPLL site, a search was made for a correlation between seismic noise level and tidal cycles, but none was detected. Since bottom currents at this site are thought to be primarily tidally driven, we infer that OBS-current interactions are not a significant source of noise. This inference is corroborated by the results of the Lopez Island experiment (see below), where there was no correlation observed between seismic noise and measured bottom currents.

The results of these investigations suggest to us that the dominant mechanism of high-frequency (> 2 Hz) noise generation at most of the sites examined thus far is of local oceanographic origin, exciting acoustic modes in the water column which couple to Stoneley modes at the sediment-water interface and waveguide modes within the sediment column.

2b. Array studies. During the 1976 Siqueiros Fracture Zone experiment (Deepsonde II), four instruments were deployed in an array consisting of a triangle with one instrument in the center (Figure 2.4). The locations of the instruments were determined using accustic transponder ranges to the ship during satellite fixes. The fix positions and OBS locations were adjusted by a least-squares scheme. The satellite data fixes were reduced using the 3-parameter short-count algorithm of Matzke (1971). The noise coherences between all possible pairs of sensors are displayed in Figure 2.5. The horizontal line represents the 95% confidence limit for the hypothesis that the true coherence is zero. Generally, at only a few isolated frequency points does the coherence exceed this level. This lack of coherence is especially surprising since one pair of sensors was separated by only 200 meters.

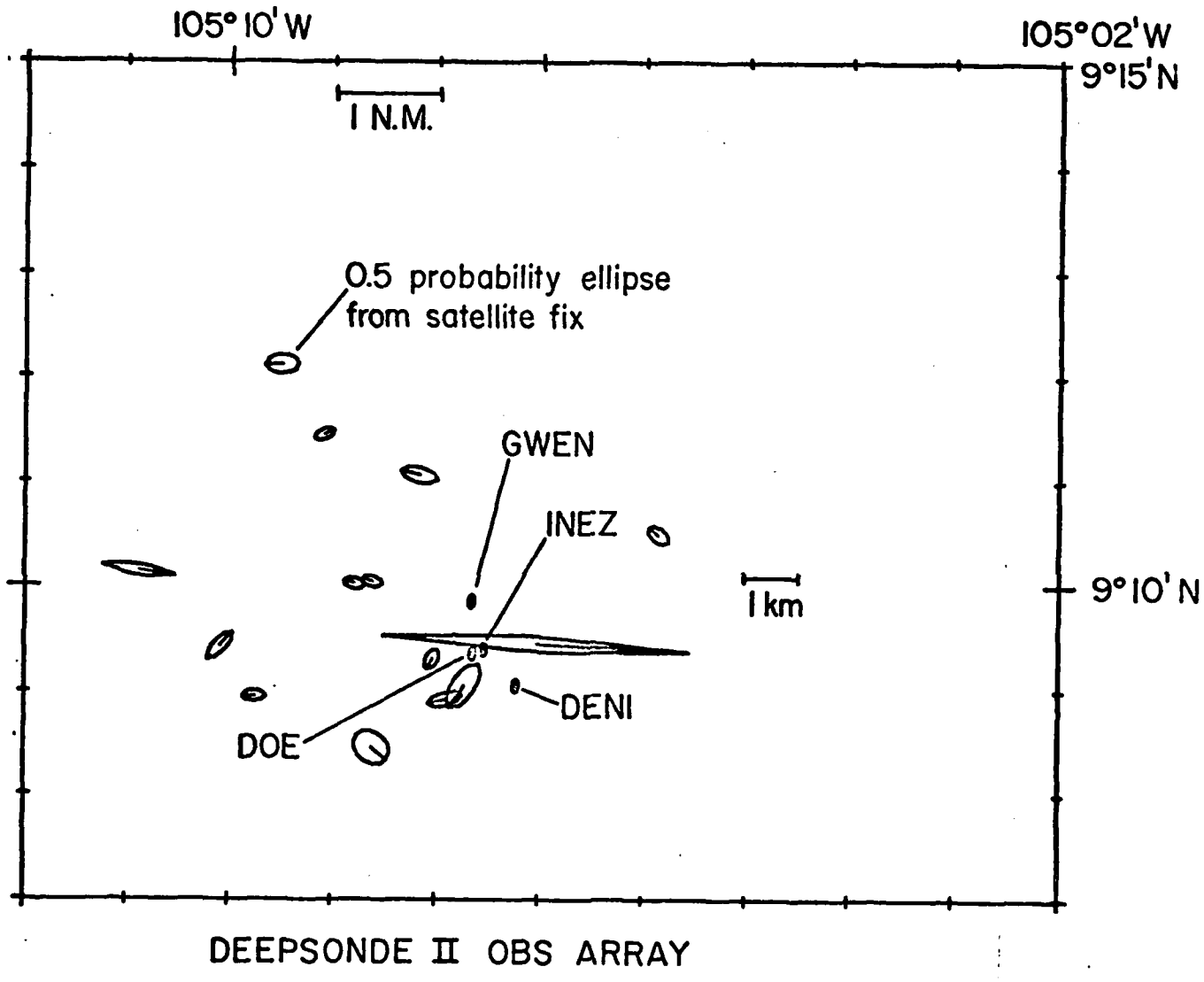

Figure 2.4. Locations and error ellipses for the four OBS's (GWEN, INEZ, DENI, DOE) in the DSII array. The other error ellipses represent satellite fixes of the R/V Washington.

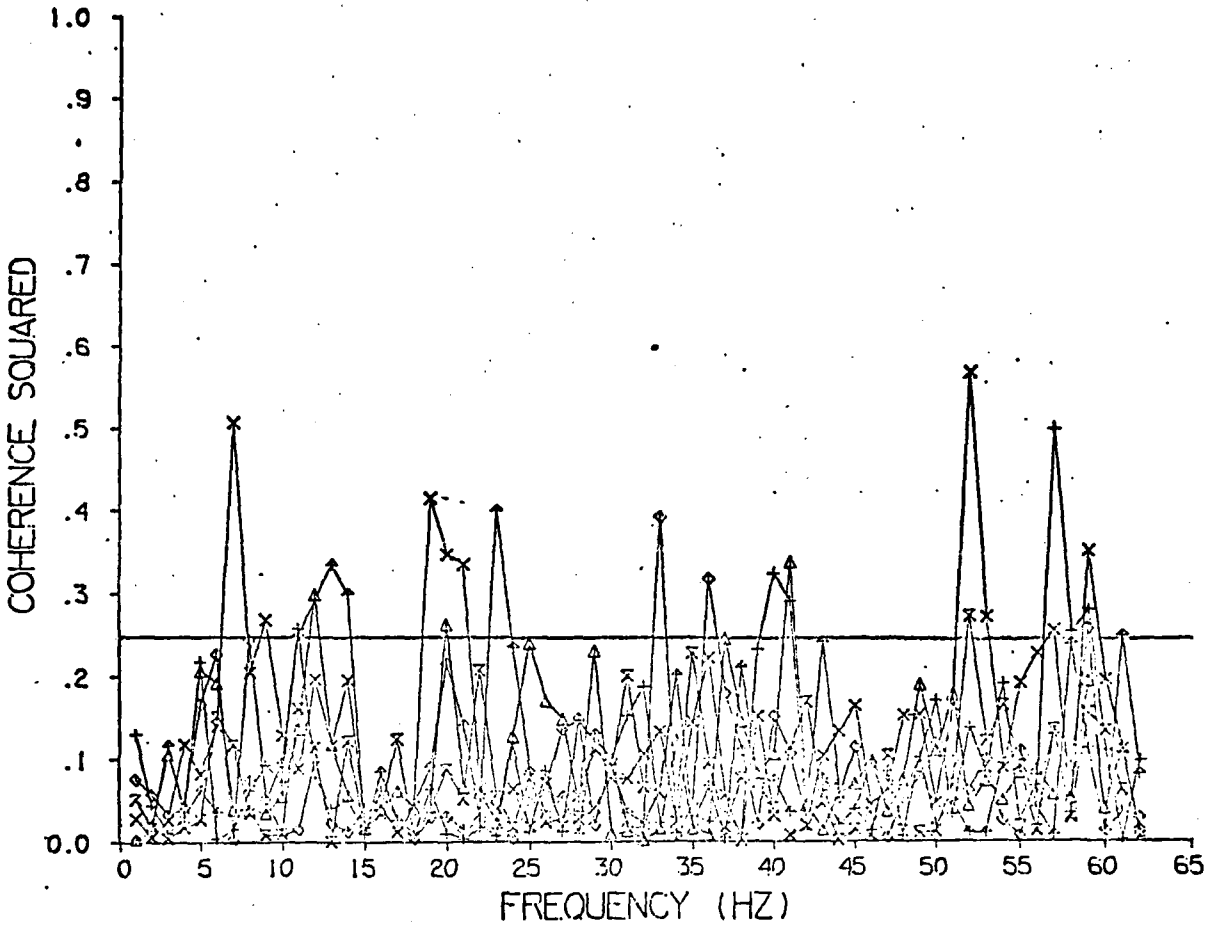

Figure 2.5. Coherence estimates for background noise observed at the DSII OBS array. Horizontal line is 95% confidence limit if true coherence is zero.

However, when the Scripps ship R/V Washington was near the array, the coherence rose to significant levels at frequencies that are multiples of the ship's screw beat (∿10 Hz).

The absence of coherence between sensors so closely spaced implies that the seismic noise must be local in origin, either concentrated in low-group velocity modes in the near-surface layers or caused by OBS-current interactions. For the reasons cited above, we favor the former hypothesis.

Similar coherence studies have been conducted for the OBS arrays deployed at the EPLL site (instrument spacing ∿ 0.8 - 1.5 km) and at Lopez Island (instrument spacing < 20 m). The results for the EPLL site were similar to those for DSII; the Lopez Island results are described below.

2c. Lopez Island experiment. During June-July, 1978, a joint OBS calibration experiment was conducted at Lopez Island in the Straits of Juan de Fuca, sponsored by the Office of Naval Research. A report under the joint authorship of the participants is currently being prepared for distribution. Here we shall outline some of the conclusions relevant to the seismic noise problem deduced by the Scripps participants, but under the caveat that these conclusions have not necessarily been accepted by the participants from other institutions.

The Lopez Island test was conducted in a small bay about 8 m deep. The data from the various OBS's (from both U.S. and foreign institutions) were cabled ashore and digitized by a multichannel system provided by Scripps. The experimental set-up is sketched in Figure 2.6. Three "standard" instruments containing 1-sec triaxial seismometers were deployed. The "plate" standard was a low-profile package which sat on top of the sediments, whereas the "spike" standard and the "neutral density" (ND) standard were buried in the sediments to enhance further the coupling and reduce further the possible action of bottom currents. The Scripps OBS was deployed in its normal tripod-mounted mode.

Typical noise spectra from the four instruments are plotted in Figure 2.7. At frequencies below 45 Hz the spectra are very similar. Although

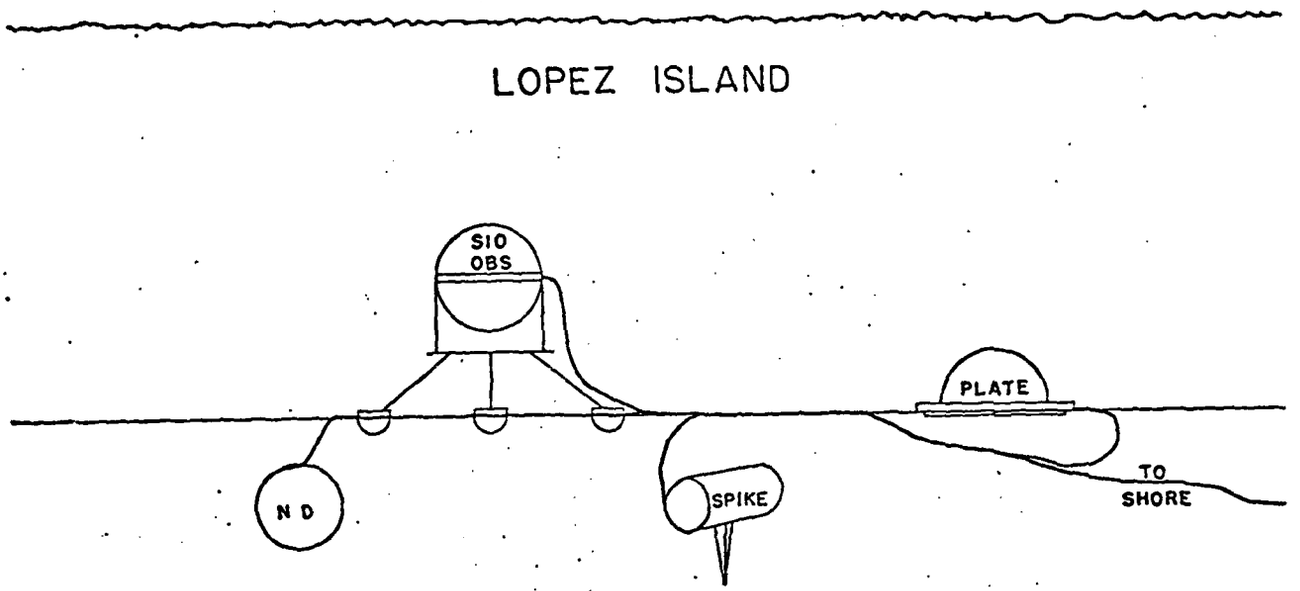

Figure 2.6. Layout of LOPEZ "calibration" experiment.

the Lopez Island site may not be typical of ocean basin environments, several conclusions derived from the experiment are relevant to this study:

(1) Recordings of various types of transient seismic signals, from low-frequency Stoneley waves to high-frequency air-gun and quarry blasts (Figures 2.8 - 2.11), reveal good fidelity in both phase and amplitude between the Scripps OBS and the standards. These observations imply that the problems of OBS-bottom coupling are not severe for instruments of the Scripps design. Our noise measurements in the deep ocean should therefore be relatively undistorted by coupling effects.

(2) The absolute noise spectra derived from the Scripps OBS and the three buried or partially buried standards are very similar, indicating that, at this site, the noise generated by the direct action of the bottom currents on the OBS package is small compared to the total noise field. This conclusion is corroborated by the observed lack of a correlation between the bottom current amplitude recorded on current meters and the seismic noise amplitude recorded on the Scripps OBS.

(3) The Lopez Island experiment provides the only data yet available from instruments spaced sufficiently closely to allow measurement of the coherence as a function of distance. The coherence between elements of the array was substantial in the same frequency band where large-amplitude, normally dispersed, low group-velocity (10-30 m/s) Stoneley waves were observed from airgun bursts, but it was very small at other frequencies. Two-dimensional wavenumber spectra computed from the array data demonstrate that the coherence lengths are short, on the order of 10-15 meters, and that most of the energy propagates towards the array from the mouth of the bay where the hydrographic disturbances are stronger.

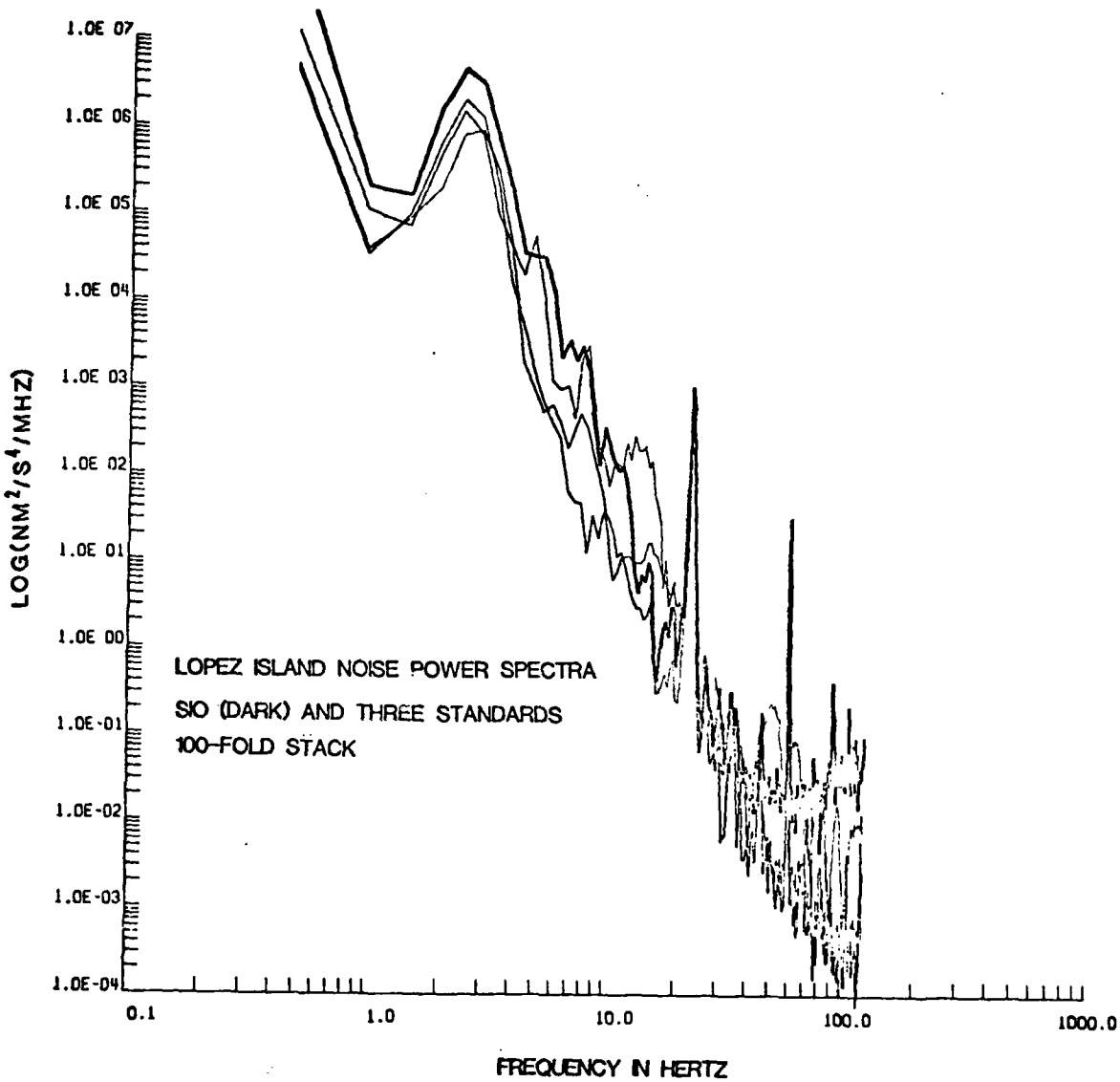

Figure 2.7. Noise power spectra from the three standards and the SIO instrument at Lopez Island. The SIO instrument is the dark line. The spikes at 60 and 22 Hz are power-line noise and noise from the R/V HOH respectively. The spectral estimates were stabilized by stacking over 100 spectra, each 512 points (~2 sec) long. The SIO instrument shows substantial electronics noise above 45 Hz.

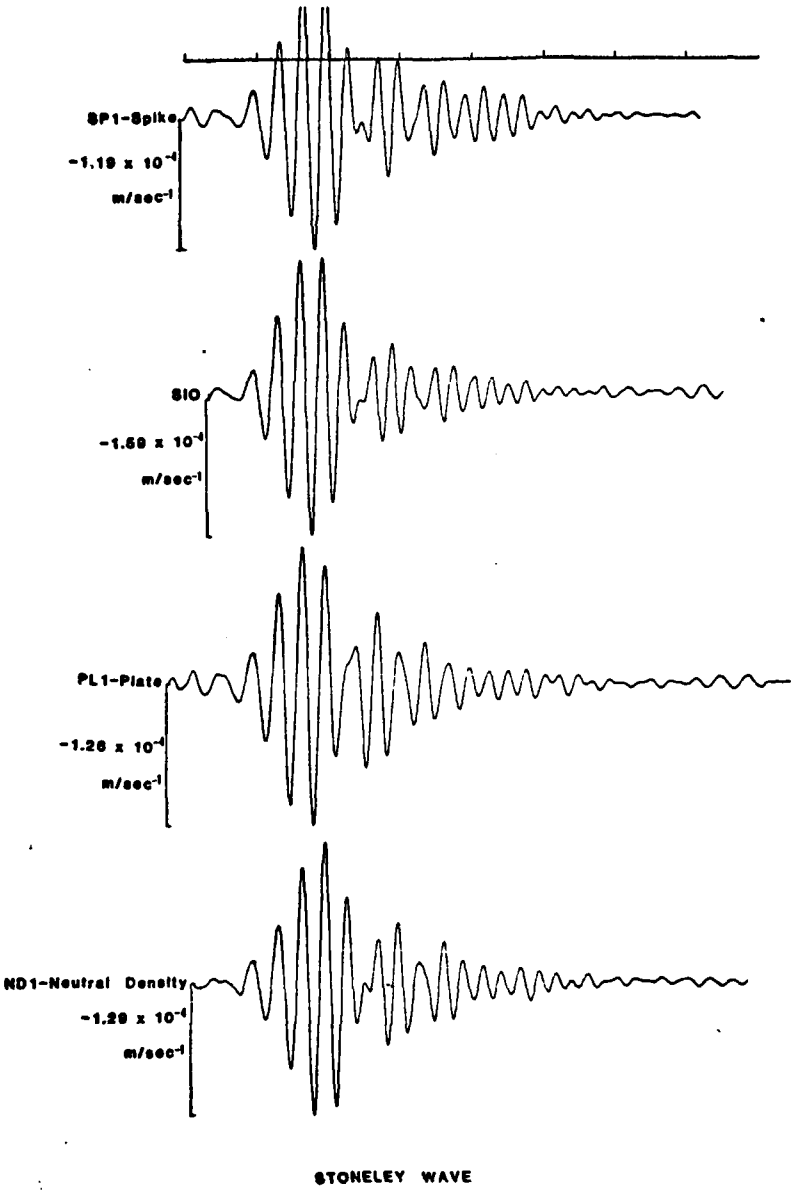

Figure 2.8. Stoneley wave recorded by SIO and three standards from Air Gun Shot 182. No filtering has been applied and the amplitudes are based on the response at 4 Hz. Note the exceptional coherence between the four instruments which indicates little cross-coupling distortion.

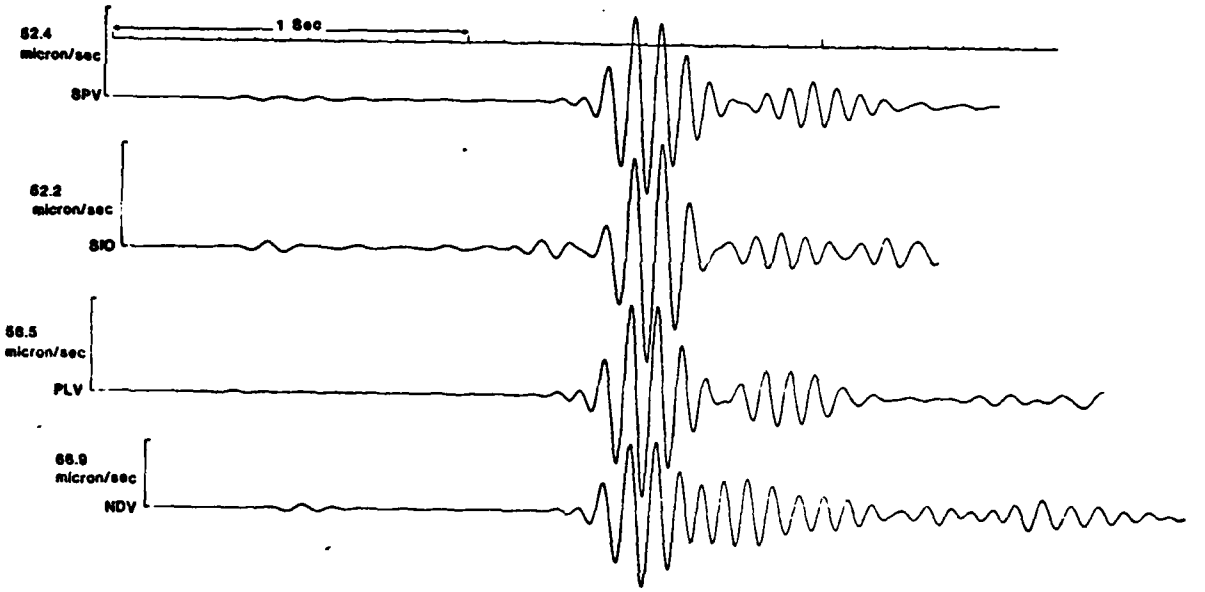

Figure 2.9. Air Gun Shot 182 recorded on SIO OBS and three standards. The records have been band pass filtered with a one octave wide, zero phase shift filter at a geometrical mean frequency of 11 Hz, the SIO "resonance" peak. The absolute amplitudes to the left were computed from the instruments' gains at 11 Hz. All the records are exceptionally coherent with NDV being the "worst" case. The absolute amplitude average of the standards is only 1.9 db higher than the SIO instrument.

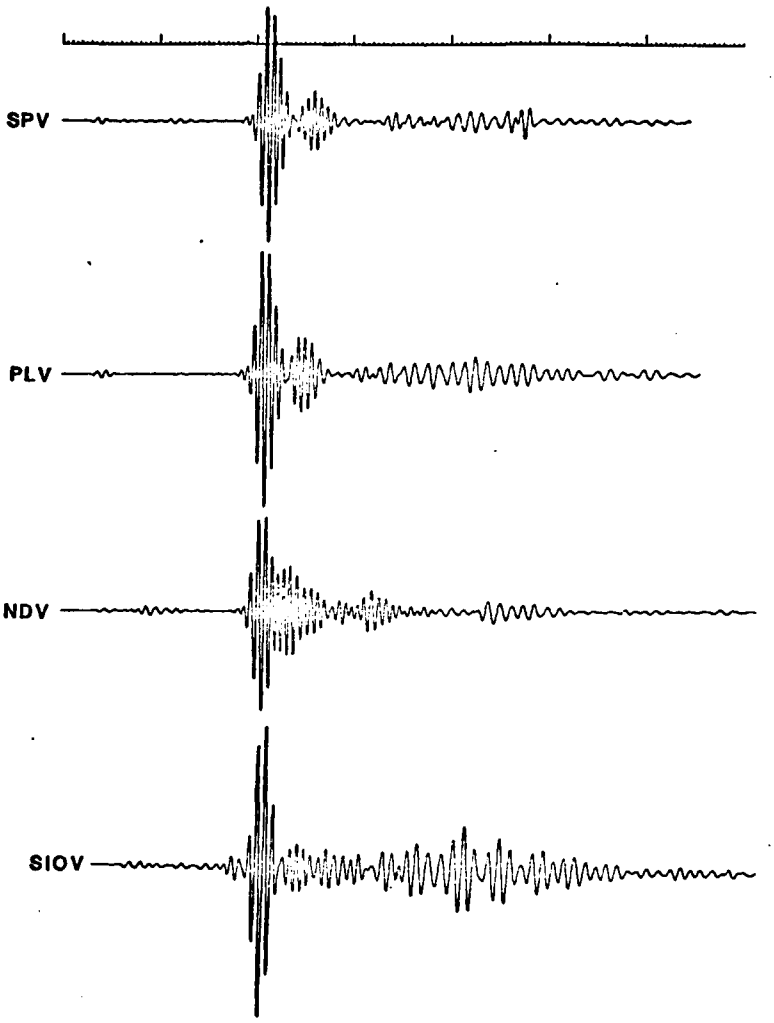

Figure 2.10. A comparison of the standards and SIO OBS for Air Gun Shot 182 between the initial arrival and the Stoneley wave. Seismograms were filtered as in Figure 2.9. Note the SIO "ring down" is shorter than the standards although the recorded shear wave is larger, indicating some cross-coupling.

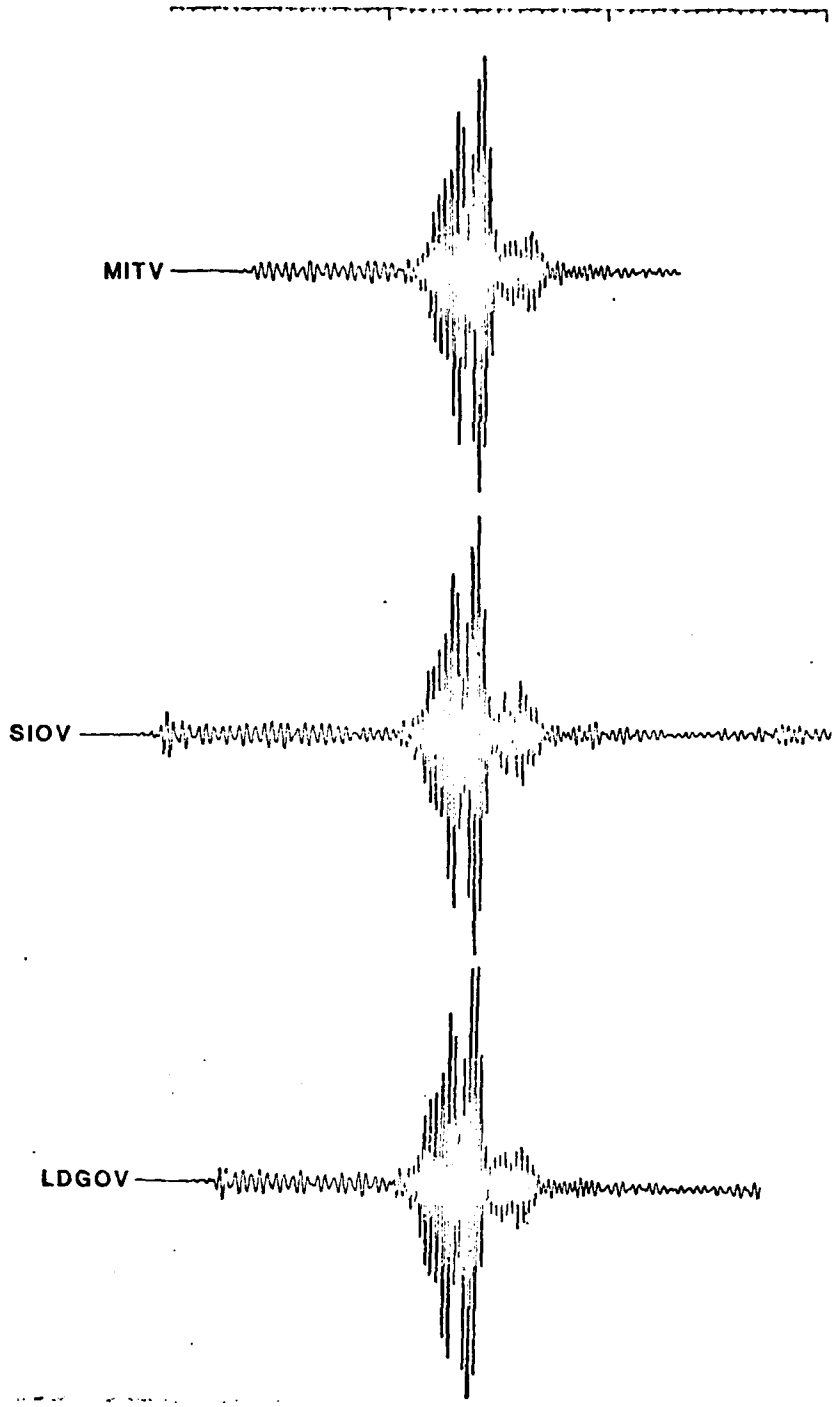

Figure 2.11. Three recordings at Lopez Island of a quarry blast at a range of >100 km. The three instruments are the MIT vertical-component OBS (MITV), the SIO vertical (SIOV) and the Lamont-Doherty vertical (LDGOV). The records were band-passed through a one-octave wide filter centered at a geometrical mean frequency of 33 Hz. The exceptional coherence of the three records implies that signal distortion due to OBS-bottom coupling is negligible at these high frequencies.

3. Middle America Trench Experiment

For the purpose of evaluating the detection and discrimination capabilities of OBS arrays we have been analyzing the records obtained by a Scripps expedition to the Middle America Trench. In the period June 6 - July 2, 1977, we operated a four-element OBS array in the Middle America Trench at 16.5°N, 100.5°W, approximately 70 km west of Acapulco (Figure 3.1). Two capsules were placed in the trench axis (GWEN and INEZ) and two were placed landward of the trench on the continental slope (DOE and DENI). Three of the capsules returned data for the entire 27 day recording period; capsule DOE returned data for only 11 days because of a trigger malfunction which exhausted her tape capacity. During the same period, a six-element land-based array was operated on shore by Mexican seismologists under the direction of Dr. Lautaro Ponce Mori in a cooperative program. Each element of the land array consisted of a vertical-component, analog-recording seismograph.

The OBS array recorded 24 events in the distance range 10-300 km and one teleseism at a distance of 83°. Preliminary locations of the local and regional events have been obtained from the OBS arrival times and from the times available to us from the land-based array. The epicenter and hypocenters of all events located by the land array for the recording period June 1 - July 10, 1977 are plotted in Figures 3.2 and 3.3. Of particular note is the SW-trending salient of activity extending seaward of the coastline; this seismicity marks the extension of a major SW-trending fault that has been mapped on land and is evidently associated with the segmentation of the subduction zone. Two events occurring in this zone were recorded by the OBS array, and their refined locations are shown in Figure 3.4. The seismograms from these two events are plotted in Figures 3.5 and 3.6.

The seismograms show complexities not observed in the land-based records of local events. One obvious complexity is the presence of compressional phases representing energy multiply reflected within the water column; these are identified by the symbol pWn in the figures. There is also a striking difference between the seismograms recorded by OBS's in the trench axis (INEZ and GWEN) and those on the sedimentary

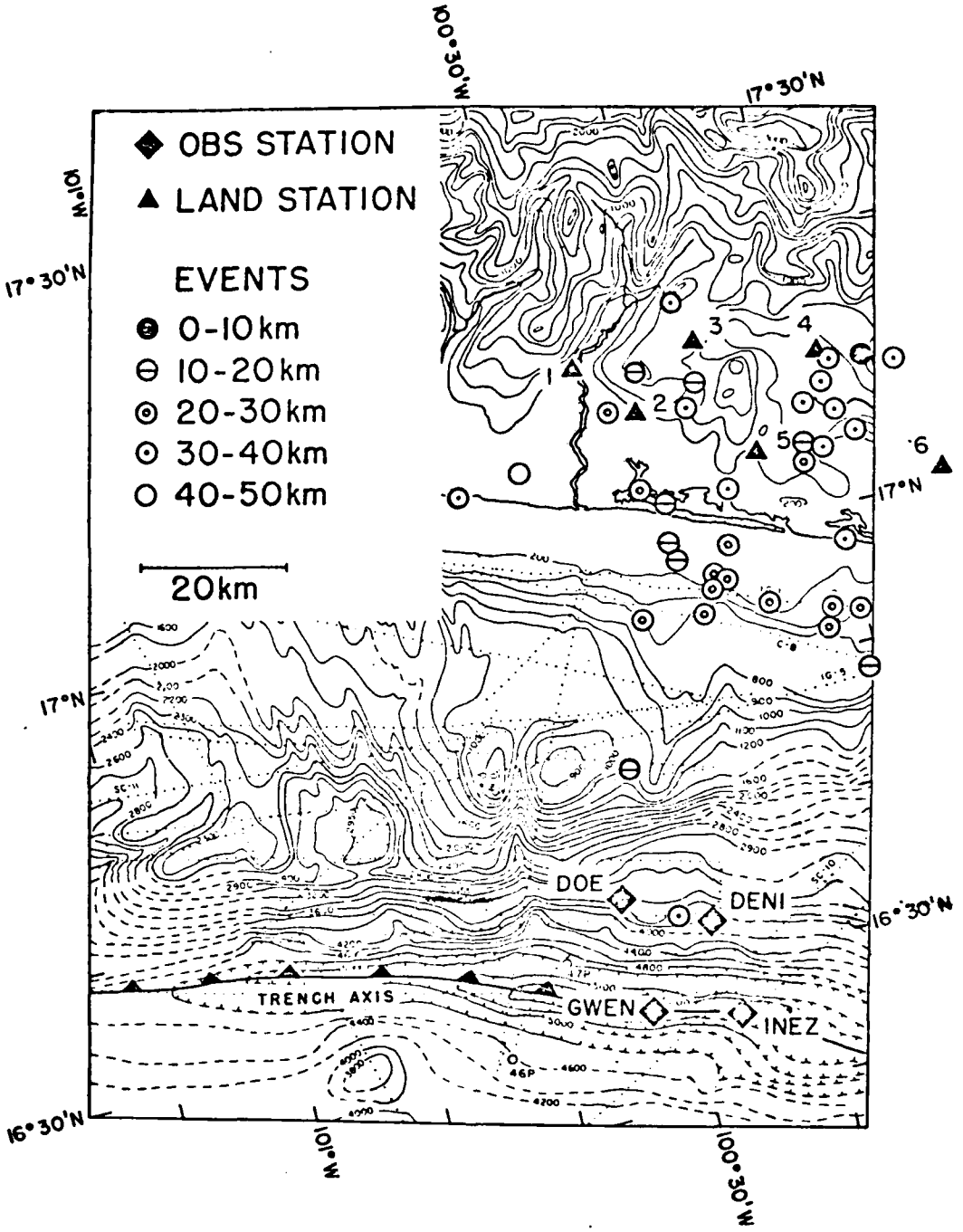

Figure 3.1. Geometry of the Middle America Trench experiment. Circles show events occurring between June 1 and June 10, 1977, located by the land-based array.

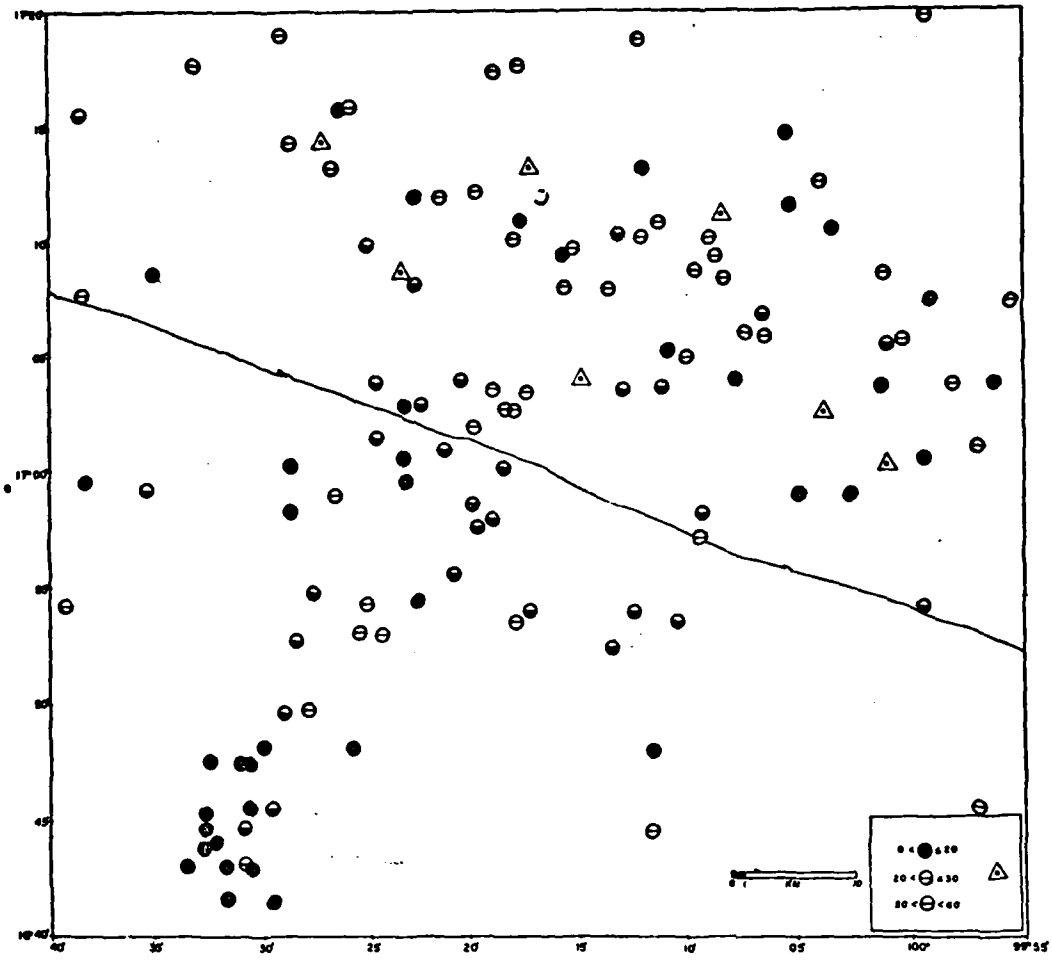

Figure 3.2. Epicenters of events located by the land array for the recording period June 1 - July 10, 1977 (circles). Triangles are land-based stations.

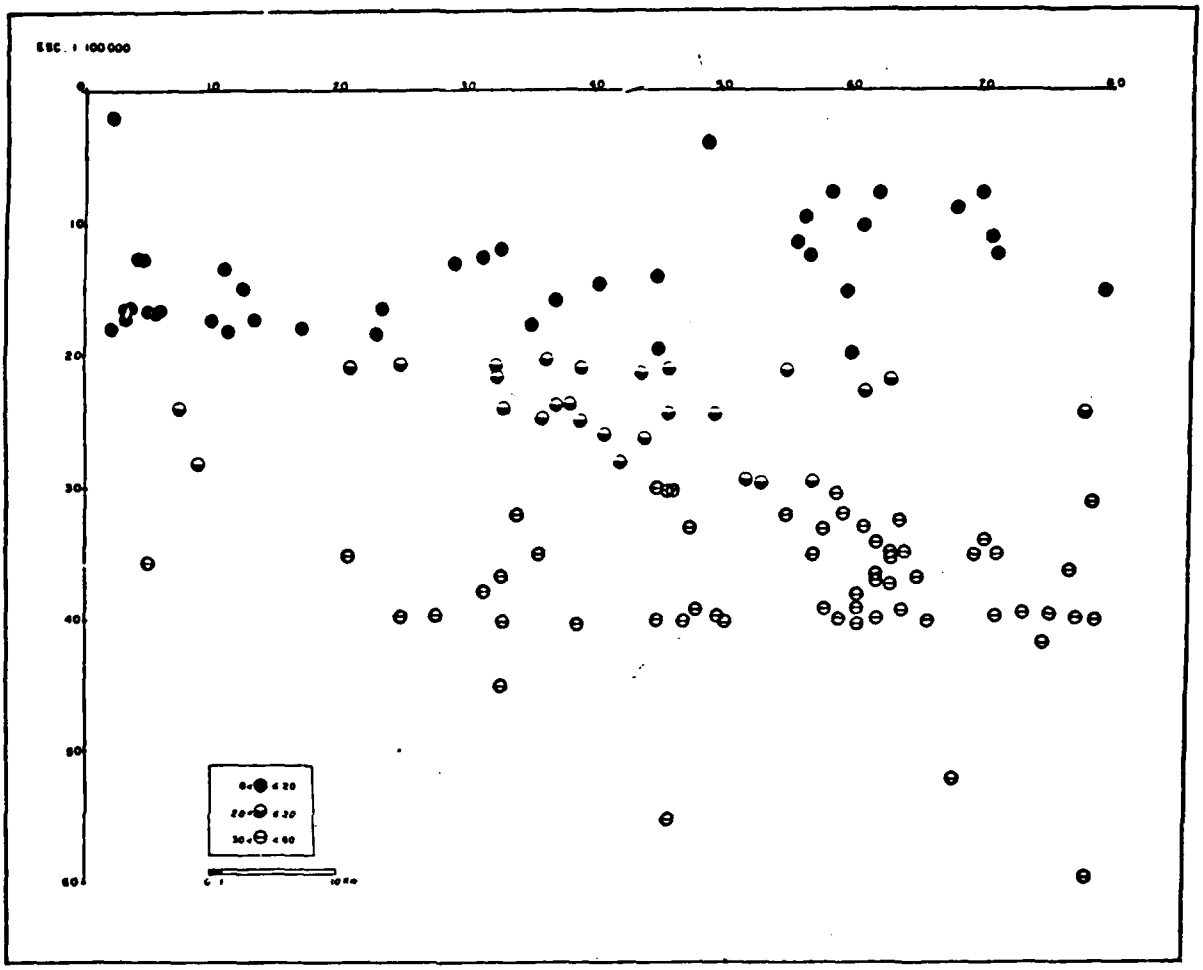

Figure 3.3. Hypocenters of events located by the land array for the recording period June 1 - July 10, 1977, projected onto a plane perpendicular to the trench.

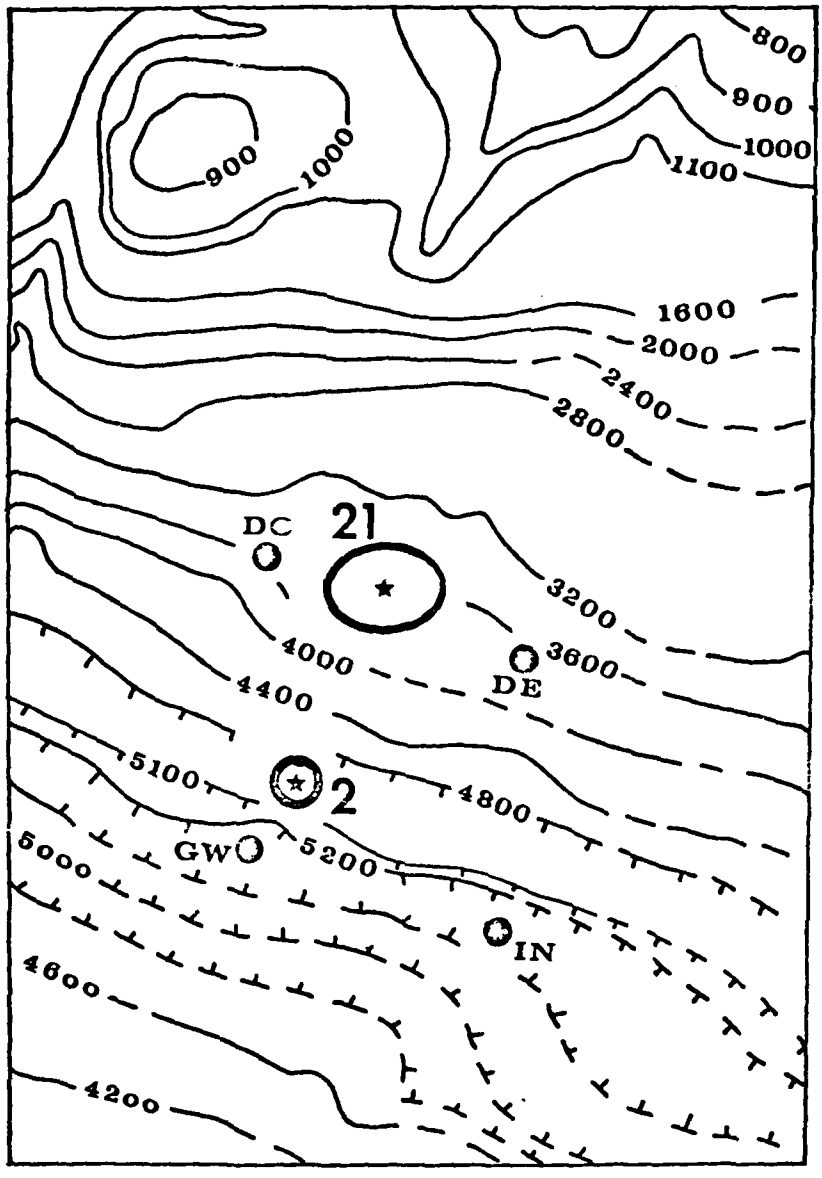

Figure 3.4. Epicenters of events #2 and #21 relative to the OBS array. Both OBS and land-based data were used in the locations. Ellipses are one standard error. The depth of event #2 is 8 ±2 km, and the depth of event #21 is 11 ±3 km.

prism (DOE and DENI). The record from DENI for event #21, for example, shows a complex, high-amplitude wavetrain following S not seen on either GWEN or INEZ. We attribute these differences to variations in sediment thickness, which varies from a few hundred meters in the trench axis to over 1500 meters at sites on the slope. At present, the exact nature of the low group-velocity modes is not well understood.

Figure 3.7 shows two records from stations in the trench axis for an event located about 160 km landward of the OBS array. Again strong water multiples, spaced at $\sim$ 7 s intervals following P, are evident on the unfiltered traces. These phases obscure the S phase, which arrives 19 s after P. However, low-pass filtering the records with a corner at 1 Hz effectively removes the water multiples, since most of their energy is concentrated above 2 Hz, and the S arrival is easily identified on the filtered traces (Figure 3.7).

Three stations of the OBS array recorded a large magnitude (M_S = 7.2) earthquake from the Tonga-Fiji region (Δ = 83.5°). The seismograms are shown in Figure 3.8 and the focal mechanism for the event is given in Figure 3.9. The OBS array lies near a node of the P-wave radiation pattern, which may account for the low amplitudes of the first motion. This event provides nearly ideal data for studying siting effects such as those discussed above. The signals for the two sites in the trench axis are reasonably coherent for at least ten seconds after P. In this interval the record from the slope site (DENI), although coherent with the other records at low frequencies, is depleted of high-frequency energy. Beginning about 8 s after P, however, energy peaked at 0.8 - 1.0 Hz emerges, eventually dominating the record. This behavior is evidently attributable to the excitation of organ-pipe modes within the thick sediment column.

Analysis of these and other earthquake records is being performed by Mr. Keith Sverdrup as part of a doctoral dissertation, which should be completed during the next contract year.

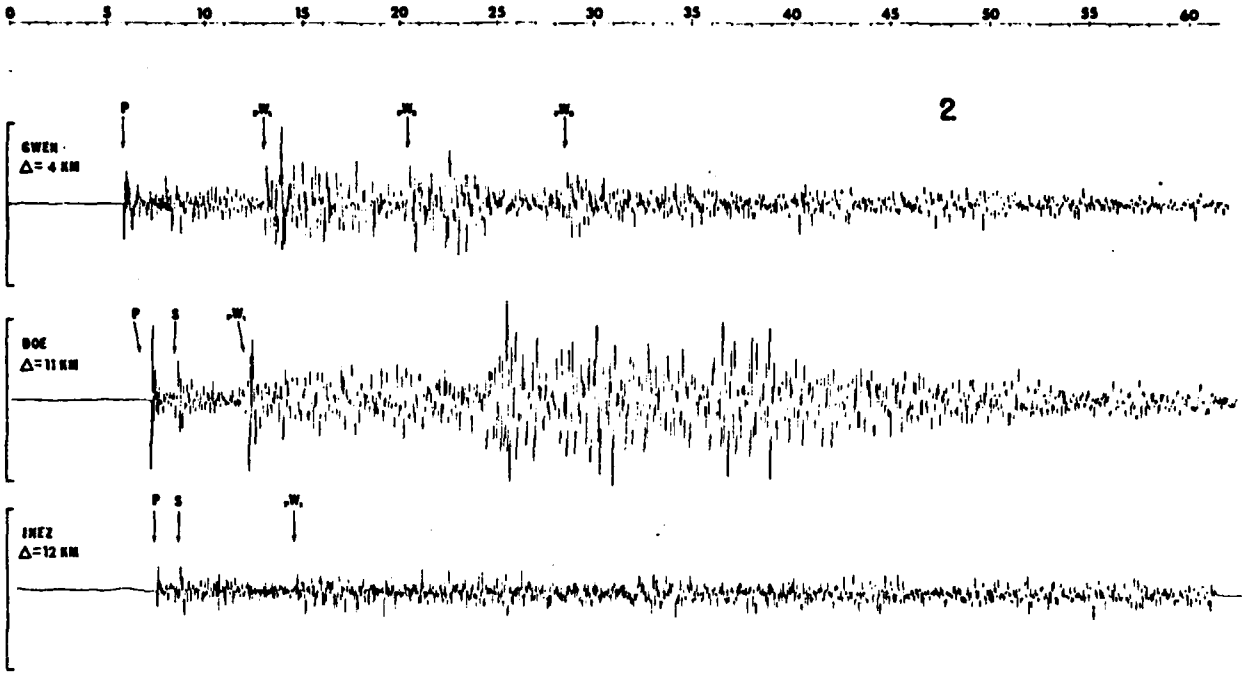

Figure 3.5. Unfiltered vertical component OBS records from event #2 on June 10, 1977, located a few kilometers west of the OBS array at a depth of about 8 km ($M_L \simeq 1$). Gains have been equalized to a common value.

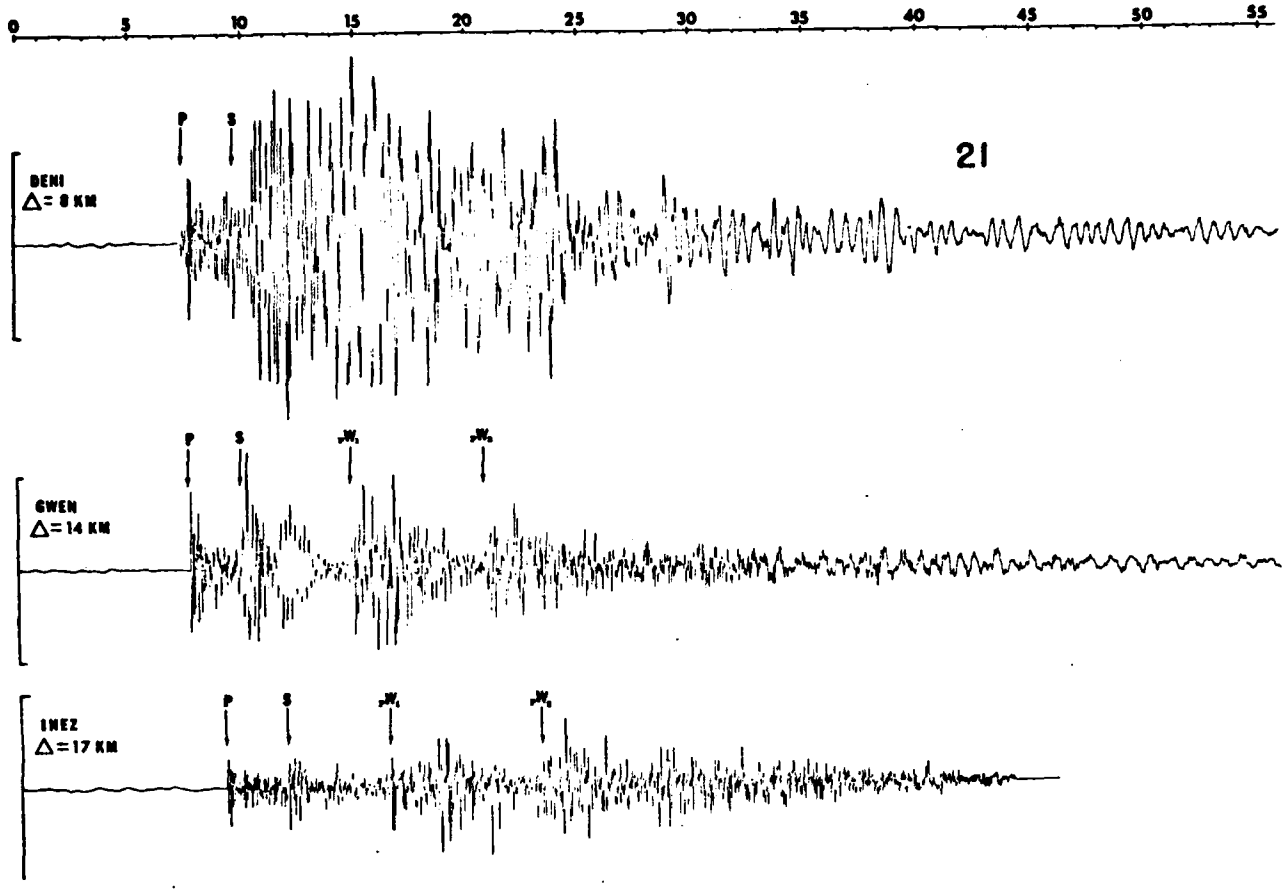

Figure 3.6. Unfiltered vertical component OBS records from event #21 on June 22, 1977, located NE of the OBS array at a depth of about 11 km ($M_L \simeq 1$). Gains have been equalized to a common value.

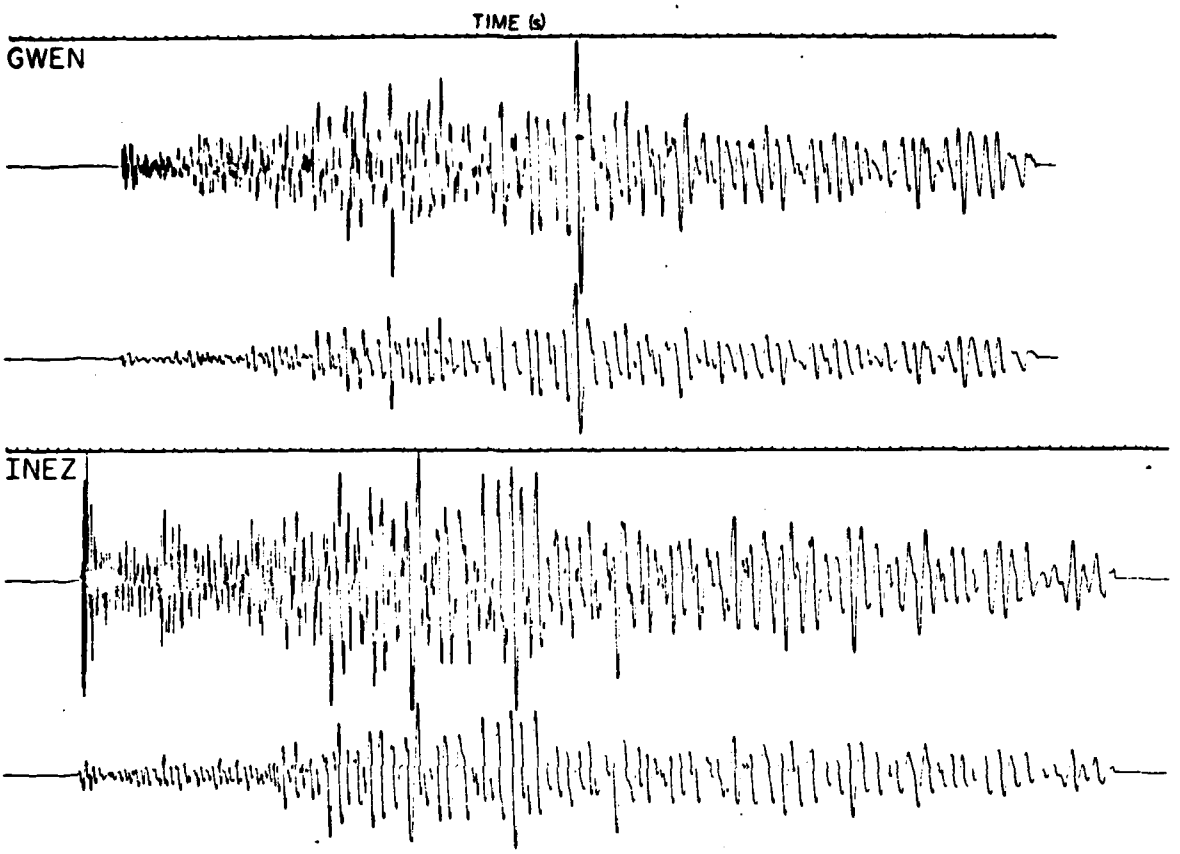

Figure 3.7. Vertical component OBS records from event #24 on June 30, 1977, located about 160 km east of the OBS array ($M_L \simeq 4$). Top record for each capsule is unfiltered; bottom record has been low-pass filtered with a corner at 1 Hz. Low-pass filtering is effective in removing the high-frequency water multiples.

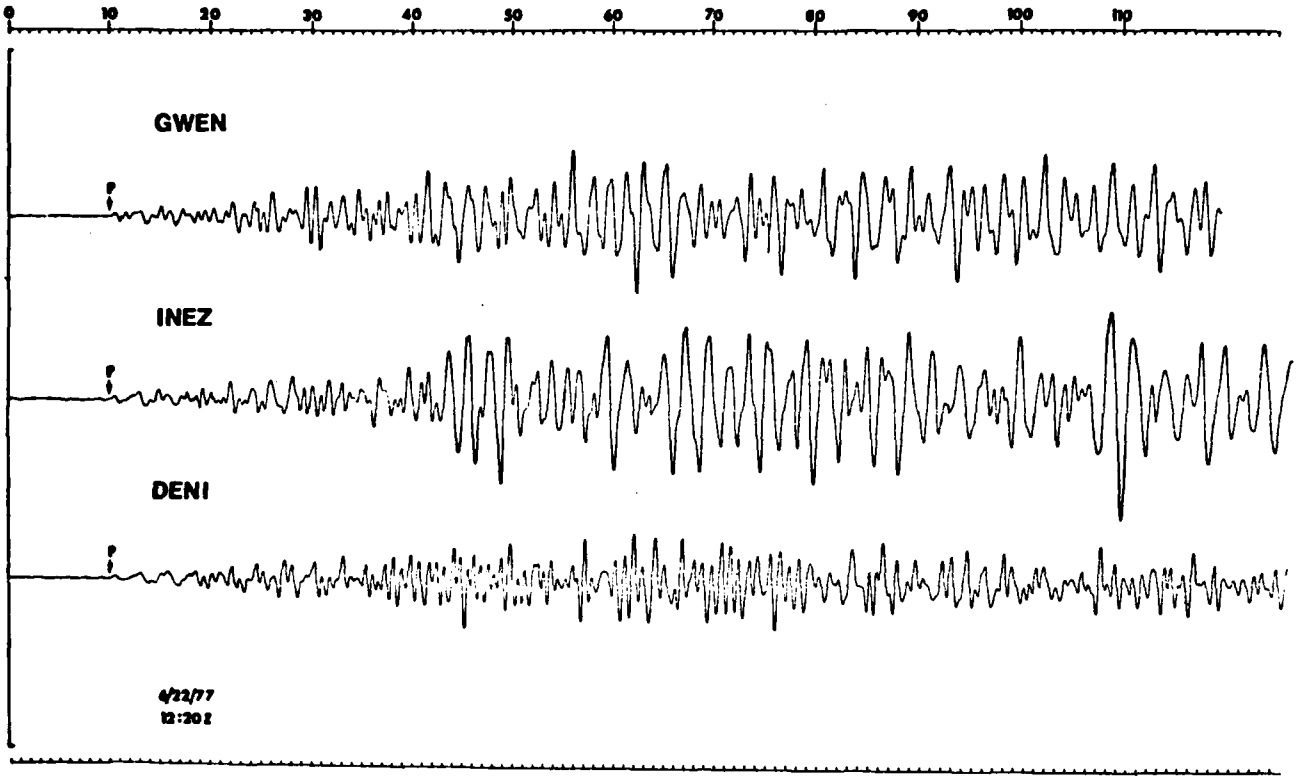

Figure 3.8. Unfiltered vertical component OBS records from event #19 on June 22, 1977, located at a distance of about 83° in the Tonga-Fiji area. This teleseism had a surface-wave magnitude of 7.2. First motion is up, representing dilatation, since the polarity of the plot is reversed from true ground motion.

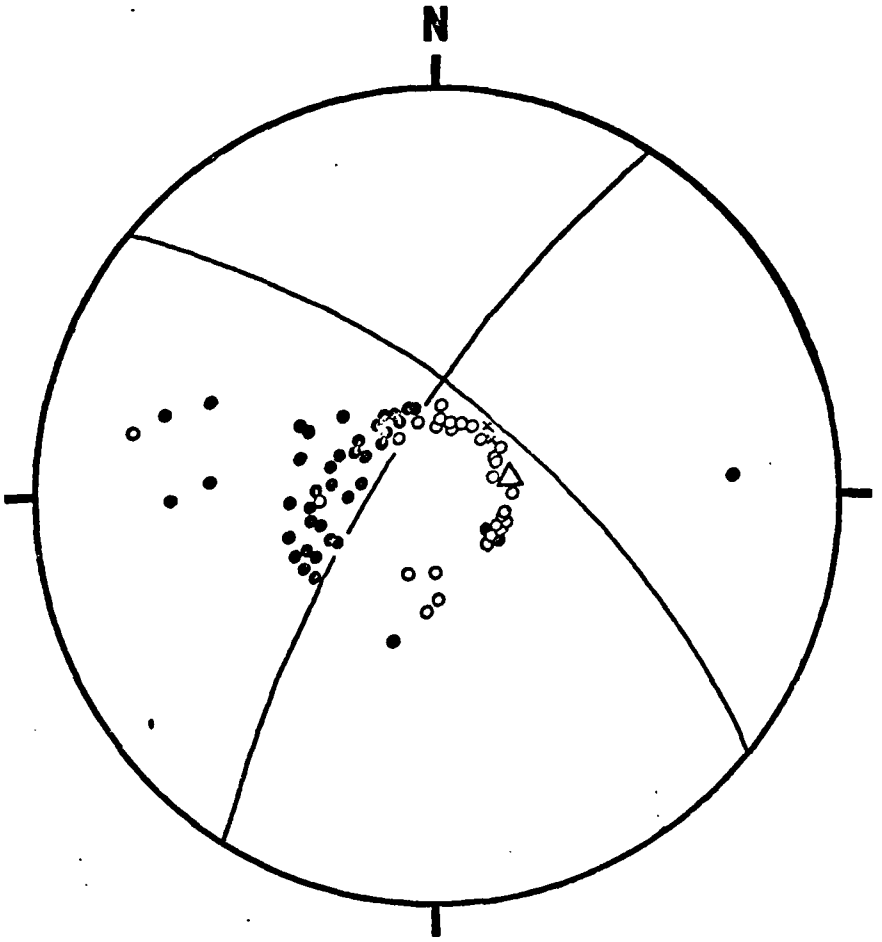

Figure 3.9. The focal mechanism for event #19 (shown in Figure 3.8). First-motion data from Earthquake Data Reports; solid symbols are compressions, open symbols are dilatations. OBS array plots as the open triangle.

4. Investigation of Triggering and Recording Strategies

4a. Triggering studies. Present technology limits us to intermittent recording of seismic data on the sea floor. An ever-present fear associated with the use of a triggered system is that of missing some event of interest because of insensitivity of the triggering algorithm.

The first step of our work has been to increase the sensitivity of the common Short Term Average/Long Term Average (STA/LTA) algorithm by tailoring the instrument response (prior to digitization) to the ambient noise spectrum (Dorman, Riedesel and Moore, 1978).

The power spectrum of background noise recorded at the ocean floor (Figure 4.1) is dominated by a peak of the resonant frequency of the seismometer. This peak is there because the seismometer response to ground displacement possesses a 'corner' in its frequency response, which is proportional to angular frequency ω above its resonant frequency and to ω^2 below it. The background noise is roughly proportional to ω^{-2} so the product of the two yields a peak or broad corner near the natural frequency of the seismometer. A peak in the instrument response is undesirable for several reasons:

(1) It limits the usable dynamic range at frequencies away from the peak because the gain must be set low enough so that the digitizer does not clip the low frequency noise peaks, thus requiring a high frequency signal to be fairly large in order to exceed the digitizer least count.

(2) The bias toward low frequencies reduces the effectiveness of simple triggering circuits such as the Short Term Average/Long Term Average (STA/LTA) ratio types. Here the LTA is dominated by the low frequency and the STA by the triggering signal. The LTA is unnecessarily large forcing the trigger to be unnecessarily insensitive.

There are several possible solutions to this difficulty. The simplest is to use a seismometer with a 5. Hz natural frequency. For work with active sources this solution is ideal, since the explosive sources contain little low frequency energy. For studies of natural events and noise, however, there is a heavy penalty paid since the low frequency performance

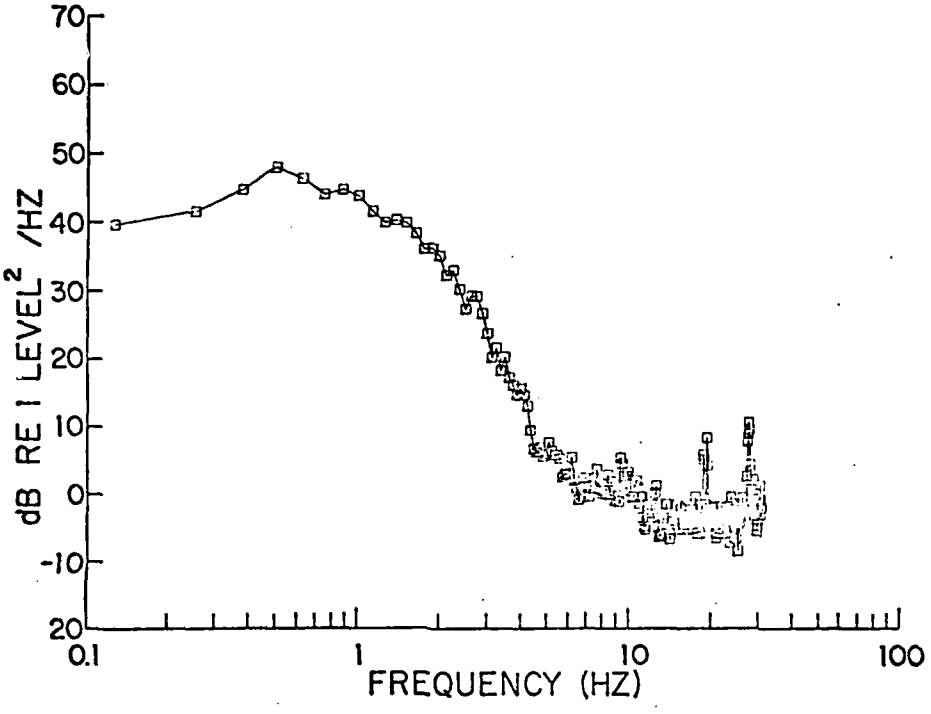

Figure 4.1. Power spectrum of seismic noise at the DSII site.

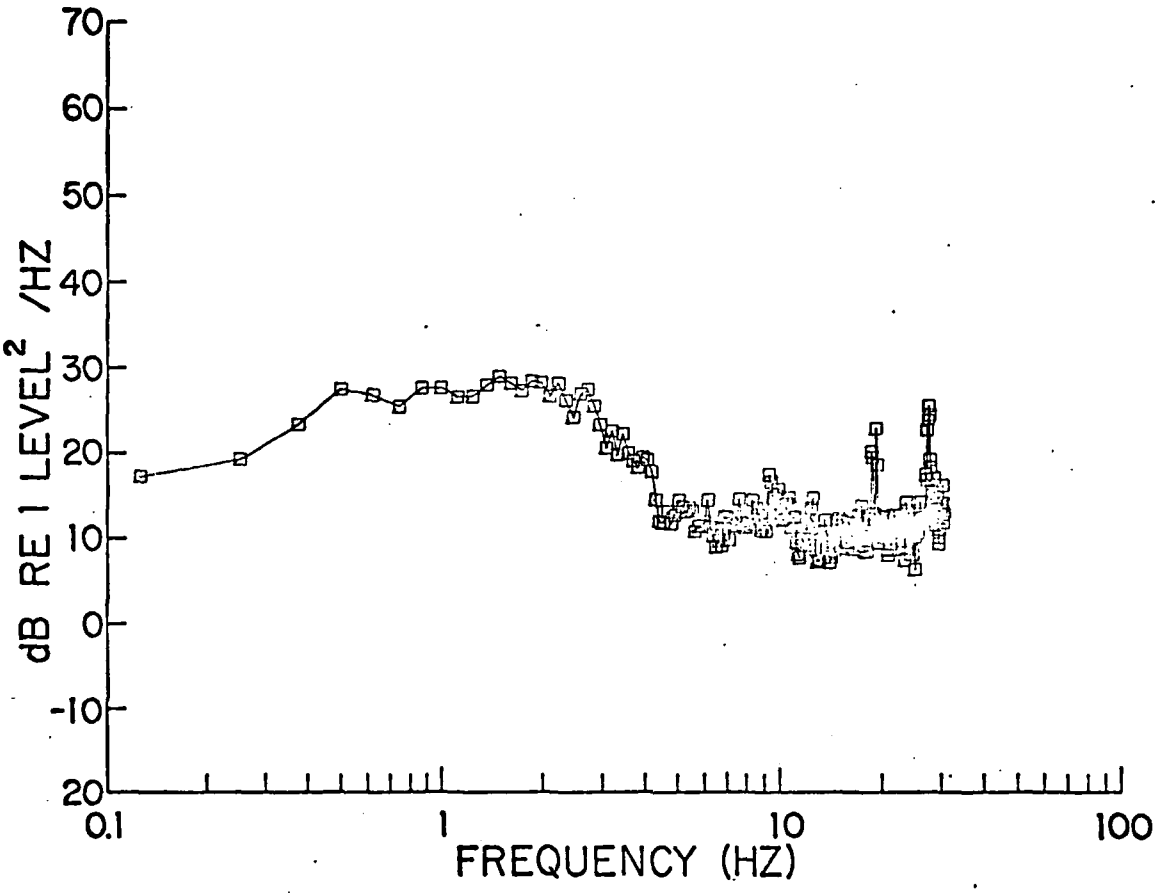

Figure 4.2. Power spectrum of seismic noise from the same data used in Figure 4.1, but taken after passing the noise samples through a pre-whitening filter to flatten the spectrum.

of the high-frequency seismometer is very poor. For this reason we have rejected this approach.

The course we have elected to follow is to use an analog filter to "prewhiten" (Blackman and Tukey, 1959) the signal prior to digitization. This process has much in common with the pre-emphasis and de-emphasis procedure used in the transmission of FM radio signals. The effect of this prewhitening filter is to boost both the high frequency and low frequency ends of the spectrum, thus flattening out the peak apparent in Figure 3.1. We have simulated this analog filter digitally and applied the recursive digital filter to data already on hand in order to insure that there were no hidden problems.

Spectra of prewhitened versions of the data used in Figure 4.1 are shown in Figure 4.2. The spectral range has been compressed by about 30 dB--from about 50 dB to about 20 dB. Rather than attempt to make the spectra absolutely flat we have purposely undercorrected.

4b. Recording methods. We have made much progress in the development of our three-component microprocessor-based ocean bottom seismographs (Moore, Dorman and Huang, 1978; Moore and Huang, 1978) and have obtained some data at sea. Because of the scheduling of our sea commitments, we have not yet run these instruments extensively on land. We have, however, begun to think about improving the total recording capacity of the instrument.

At the present state of the art the only practical recording medium available to record data in the quantity required in an OBS application is magnetic tape. In the microprocessor OBS a high quality reel-to-reel audio tape transport, using 1/4" tape, modified for digital recording, is used. Data are recorded serially on four tracks at a bit density of 1843.2 bits per inch. The recorder can handle 5" diameter reels resulting in a tape capacity of about 1800' of 1/2 mil tape. This results in a total recording capacity of about 159 megabits, and a total data recording time of 6.4 hrs. at the 15/16" per second tape speed used. The present system uses a scheme, known as "bi-phase-level" (BØL) encoding to record the digital data on the tape. This system performs extremely well,

considerable testing indicating a random bit-sensor rate, apart from tape drop-outs less than $1:10^7$ bits. This work has suggested that it should be possible to increase the total storage capacity by at least a factor of 4, still maintaining the present low random error rate. Before describing the work in progress, a quick general discussion of digital recording techniques is presented in order to clearly define the terms used in the discussion of the work proposed.

The general problem of recording digital data on magnetic tape reduces to the problem of recording a simple serial string of ones and zeroes on the tape and later recovering it. This is true even in the case of standard computer tape formats (either 7 or 9 tracks) as the playback process is essentially a matter of recovering the single serial bit stream represented by each track. The first step in recording the data is to convert the data being recorded from a series of "words," in our case 12 bits long, into a continuous stream of bits output at some terminal at a uniform, steady rate. What then appears at the terminal is a series of voltage levels, one level representing zero, another representing one, corresponding to the bit series being output. The timing of this operation is controlled by a "clock." The clock is a square wave at some frequency (in the current system 1728 Hz). At particular transitions of the clock (either each positive transition or each negative transition) a new bit appears at the terminal. The dwell time of a bit at the terminal is called a bit-time, and the clock is called the bit clock. A bit stream of this type which is essentially a varying voltage where the level during each bit-time determines whether the bit is 1 or 0 is coded in non-return-to-zero (NRZ) format. Coding in the sense used here means producing a waveform in which the behavior of the voltage signal during a bit-time determines whether the given bit is a 1 or a 0. The choice of coding scheme used is governed by the requirement that the waveform is ultimately recorded on the tape, considering both the properties of the tape recording and playback process and the problem of reconstituting the original NRZ bit stream from the waveforms produced by playing back the tape will result in a low error rate.

For practically any conceivable code a knowledgeable person could reconstruct the original series of bits by examining the waveform obtained upon playing back the tape if he knew where the bit boundaries were; i.e., the bits could be determined by examining subsequent segments of the reproduced waveform between bit boundaries. Thus the reconstruction of the encoded bit sequence from the waveform obtained by playing back the tape is possible only if the clock can be reconstructed, properly phased with respect to this waveform. This is really the fundamental problem to be solved by any coding-recording-playback scheme.

Two particular coding schemes are being investigated; BØL, mentioned before and presently used, and a scheme known as NRZ mark (NRZM). Figure 4.3 represents both these coding schemes. The top line shows a typical bit sequence output by the computer. The next line is the square wave used to clock the process. A new bit is "clocked out" on each new clock transition. The next line shows the bit sequence represented in NRZ form by a voltage jumping between 0 level and one level. This waveform is that at the terminal in the discussion above, each bit residing there for one bit-time. The next line is the corresponding BØL code. In this code a one is represented by one cycle of the clock (Ø) during the corresponding bit time and a zero by one cycle of inverted clock (Ø). An advantage of this scheme is that, regardless of the bit pattern recorded, a bit-clock of the proper frequency whose phase relative to the "time" bit clock is definite may be reconstructed from the play-back waveform by phase-lock-loop (PLL) techniques. This code is thus said to be "self-clocking." When this code is used, the tape is recorded by applying a current, with the waveform of line 4, to the record head. Each of the transitions of line 4 causes a reversal of the flux impressed thereby on the tape. The system problems due to the tape recording and playback process are a function of the density of flux reversals on the tape, not of the bit density per sec. That is, a coding scheme with a larger number of flux reverasals per bit has a lower maximum bit density than one with a smaller number of flux reversals per bit. For BØL code the average number of flux reversals per bit is between 1 and 2 (for random data, 1.5).

Line five of Figure 4.3 shows the coded waveform for NRZM. In this scheme, a transition (either + or -) at the beginning of a bit time represents a 1, no such transition a zero. Note that in this scheme, line six, labeled NRZM' represents exactly the same bit sequence as line five; i.e., only transitions, not their direction, are important. Again, it is easy to reconstruct the original bit sequence corresponding to line five or six if the locations of the bit-time boundaries are known. However, this code is self-clocking only if the recorded sequence is sufficiently rich in 1's. (In the case of a long sequence of zeroes, no waveform is recorded at all!) The attraction of this code is the fact that for random data the average number of flux reversals per bit is 1/2; i.e., from a given record-reproduce scheme it can be recorded at bit densities three times the maximum obtained using BØL.

The self-clocking problem can be solved in a number of ways. One method is to insert check bits into the bit stream at regular intervals. For example, one could insert a bit, every four bits, such that the sum of it and the preceding three is always odd (odd penalty). This insures at least one transition every four bits. The drawback of this is that only 75% of the tape is data, the remaining 25% being overhead. The check bits can be generated by more sophisticated means such as error-deletion polynomials. These techniques provide the potential of correcting bit errors in the group of bit checks unambiguously. They can provide enough information to correct single bit errors, double bit errors, etc., up to the point where all the bits in the checked group can be unambiguously reconstructed. The greater the error counting potential, the greater the overhead. In the case where all bits can be reconstructed, the check character contains more bits than the data character.

We are now mounting a coordinated attack on the tape recording problem at several points with the goal of increasing the total storage capacity significantly with no increase in error rate. The points of attack are:

(1) Increase of recorded flux reversal density. The present scheme is quite conservative and an increase of at least a factor of two can be made here.

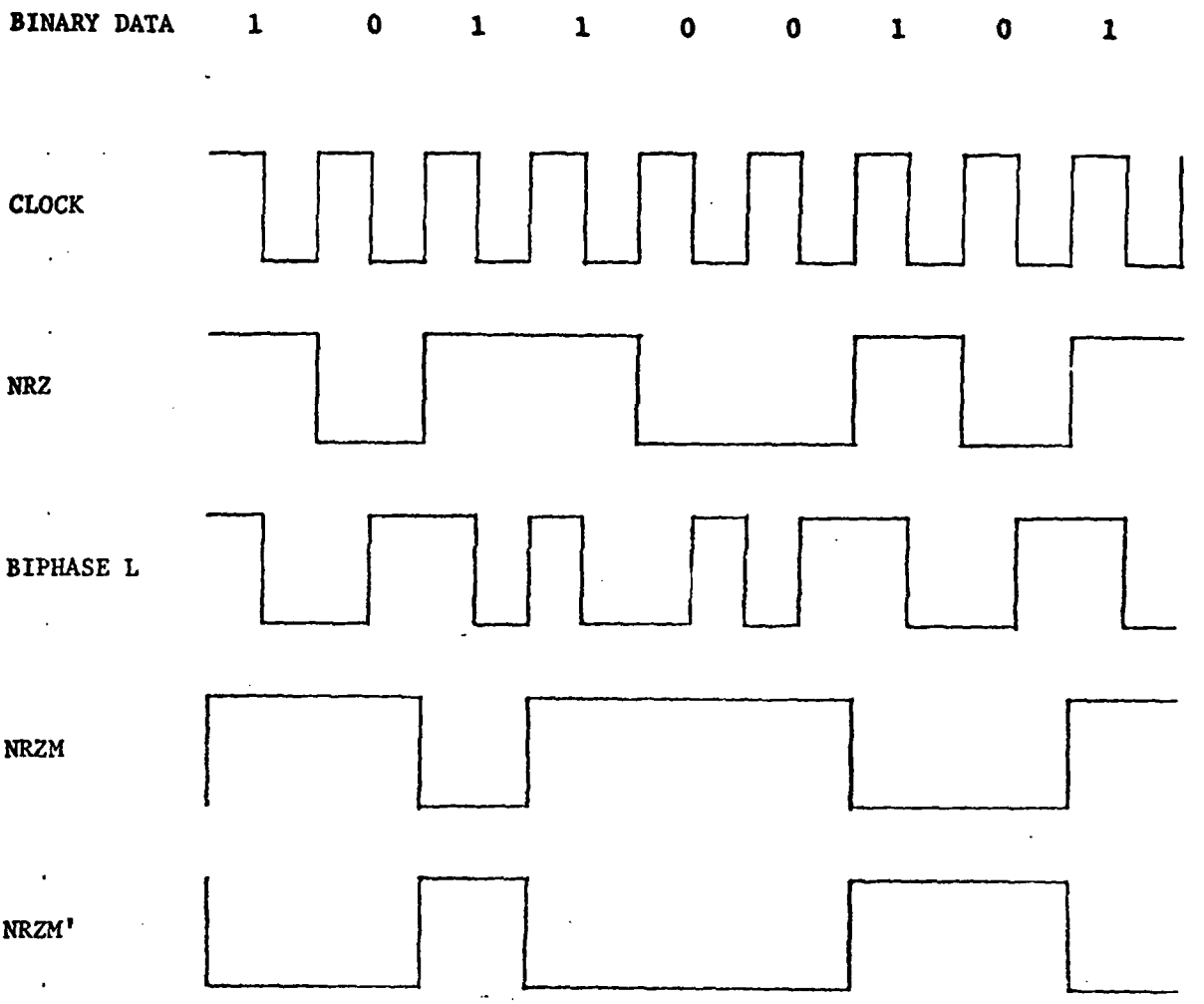

Figure 4.3. Graphs of flux transitions recorded on tape using biphase and Non-Return-to-Zero (NRZ) encoding schemes to record the binary signal 101100101. Note that the biphase encoding requires about twice as many flux transitions as do the NRZ codes.

(2) Choice of an optimum self-checking scheme that will provide maximum error correction for a given overhead.

(3) Implementation of a tape playback scheme that does not use a PLL. This will have the effect of making the data loss due to transient disturbances such as tape drop-out much smaller.

References

Achenbach, E., Vortex shedding from a sphere, J. Fluid Mech., 62, 209-221, 1974.

Blackman, R. B., and J. W. Tukey, The Measurement of Power Spectra, Dover, New York, 190 pp., 1959.

Dorman, L., M. Riedesel, and R. D. Moore, Prewhitening applied to ocean bottom seismology, EOS, 59, 1131, 1978.

Hughes, B., Estimates of underwater sound (and infrasound) produced by nonlinear interacting ocean waves, J. Acoust. Soc. Amer., 60, 1032-1039, 1976.

Matzke, D. E., An optimum six parameter estimation process for navigation satellite (SRN-9) data, Mar. Tech. Soc. J., 5, 37-42, 1971.

Moore, R. D., L. M. Dorman, and C.-Y. Huang, Scripps' microprocessor ocean bottom seismograph, EOS, 59, 1131, 1978.

Moore, R. D., and C.-Y. Huang, Microprocessor-based ocean bottom seismometer, Proceedings of the Digital Equipment Computer Users Society (DECUS), 781-786, San Francisco, November, 1978.

Phillips, J. D., and D. W. McCowan, Ocean bottom seismometers for research: a reassessment, Technical Note 1978-40, Lincoln Laboratory, Lexington, Mass., 1978.